NITRIC OXIDE TRIGGERED DEPHOSPHORYLATION REACTIONS

by

EMEKA MARTIN ENEMCHUKWU

Submitted in fulfillment of the requirements
for the degree of

MASTER OF SCIENCE

in the subject

CHEMISTRY

at the

UNIVERSITY OF SOUTH AFRICA

SUPERVISOR: PROF F TAFESSE

JANUARY 2009

DECLARATION

I, Emeka Martin ENEMCHUKWU sincerely and solemnly declare that the work: **NITRIC OXIDE TRIGGERED DEPHOSPHORYLATION REACTIONS** is my work and that all sources quoted have been indicated and acknowledged by means of complete references.

DEDICATION

This research dissertation is dedicated to the will of the Almighty God, to my loving parents, Mr. and Mrs. Ambrose Grace Enemchukwu and to all who believe in the oneness of humanity.

ACKNOWLEDGEMENTS

My sincere gratitude goes to my supervisor Prof. Fikru Tafesse not only for initiating the project but for being the fatherly figure I so much adore in my times of worries and tribulations during the course of this research. Sir, words and letters can never express how I feel towards your unalloyed support for us your post graduate students.

I would like to thank Prof. Jack Malose Mphahlele for not losing faith in my abilities and providing me with the privilege and opportunity to have a taste of higher education even in the midst of some unfounded obstacles. Sir I want you to know that you are and will always remain my mentor.

To the mother I will always cherish, Prof S.O. Paul. Mum in those confusing moments I always relied on your reassuring smile of hope to put me through daily and to keep me going. *Merci maman*.

I would also like to thank Prof. Ifeanyichukwu H. Atagana for taking me as his own child. Papa I will always be your son. I sincerely thank Raymond Anyasi for being my brother, Eguzozie Kennedy for being my support and my critic and to Elochukwu Enemchukwu for raising my hopes and aspirations. I will also like to say thank you to Tluo Makwakwa for always listening and to Ubani Onyedikachi for being a good companion. Lest I forget, Gilbert, Mark, KC, Nnamdi, Deliwe and Lenette, I owe you guys a lot.

My sincere gratitude also goes to the Department of Chemistry, College of Science, Engineering and Technology and the University of South Africa for the financial assistance extended to me in the form of post graduate academic assistantship. Above all I give glory to God.

ABSTRACT

The synergistic effect of nitric oxide toward dephosphorylation reactions involving phosphate esters was the subject of investigation in this research. Sodium nitroprusside under UV irradiations at 254nm, 365nm and white light was utilized as nitric oxide donor in solutions. The effects of cobalt trimethylenediamine and nitroprusside towards dephosphorylation of nitrophenylphosphate and pyrophosphate which were modeled as organophosphate ester substrates were also investigated. The activated substrate models showed more rate enhancement than the unactivated models in all cases. The direct interaction of nitric oxide with the phosphorus centre is presumed to be the reason for enhanced hydrolysis. This study demonstrates the possible role of nitric oxide in decontamination reactions of poorly biodegradable phosphate esters in the biosphere.

KEY TERMS: Nitric oxide, nitrophenylphosphate, sodium nitroprusside, phototransformation, decontamination, dephosphorylation, inorganic phosphate, inorganic pyrophosphate, nitrophenolate ion, trimethylenediamine, organophosphate esters, ultra violet radiation.

TABLE OF CONTENTS

CHAPTER TWO

CHAPTER THREE

LIST OF ABBREVIATIONS

AChE	Acetylcholinesterase
ATP	Adenosine 5'- triphosphate
cGMP	Cyclic guanosine monophosphate
DNA	Deoxyribonucleic acid
EDRF	Endothelium derived relaxation factor
en	Ethylenediamine
GTP	Guanosine triphosphate
NDP	Nucleosidase 5'- diphosphate
NPP	4-nitrophenylphosphate
NTP	Nucleosidase 5'- triphosphate
NP	P-nitrophenol
PAP	Purple acid phosphatase
PPi	Inorganic pyrophosphate
Pi	Inorganic phosphate
SNP	Sodium nitroprusside
tn	1, 3 diaminopropane
UVA	Near ultraviolet (320nm-400nm)
UVB	Middle ultraviolet (280nm- 320nm)
UVC	Far ultraviolet (180nm-280nm)

LIST OF TABLES

LIST OF FIGURES

LIST OF REACTION SCHEMES

CHAPTER ONE

1.0 INTRODUCTION

Dephosphorylation reactions of organophosphate esters are of crucial importance in biological systems. This class of esters are involved in energy transduction, biosynthesis, and control of secondary messengers as well as regulation of protein function. Inevitably, a wide range of enzymes have evolved to catalyse this deceptively simple reaction, operating via a range of different mechanisms and under a wide range of different conditions. Thus, there are enzymes that function in high and low pH, and utilise direct attack by water or employ an enzyme-derived nucleophile [1]. Phosphate ester dephosphorylation has also become the focus of much effort in the design of artificial catalysts [2, 3] many of which draw inspiration from known enzyme structures. All these efforts are geared towards reducing environmental problems posed by organophosphate ester compounds which in one way or the other promote pollution in the environment. Furthermore, there is also a need to understand the mode of reactivity of this class of esters in biological systems and the ecology at large. Some class of organophosphate esters commonly used in insecticide formulation are mostly nerve poisons and may cause cumulative damage to the nervous systems and liver. They can also be carcinogenic. In the aquatic environment, they accelerate the eutrophification of surface waters causing increased growth of undesirable algae and aquatic weeds. This results in shortages of dissolved oxygen in water systems, massive bloom of cyanobacteria, fish kills, foul smells, unpalatability of drinking water and the formation of trihalomethane during water chlorination in treatment plants [4] to mention but a few. Some organophosphate esters find various applications that range from being used in fertilizer formulations, pH stabilizers and water softeners in water treatment plants. This wide range of uses makes dephosphorylation studies an important aspect in organophosphate ester studies. Catalytic and stoichiometric dephosphorylation studies of organophosphate ester models involving metal complexes in different reaction media have been advanced in the literature [5-8]. Our current study focuses on the involvement of nitric oxide as a trigger in the

dephosphorylation reactions involving organophosphate esters. It investigates the effects of nitric oxide in the dephosphorylation reactions by monitoring the amount of nitrophenolate ions and inorganic phosphate produced in the reaction. It is also designed to study the synergistic cooperativity between nitric oxide and cobalt (III) ions in the dephosphorylation of phosphate ester contaminants in the environment. A brief description of organophosphates in the environment is discussed below.

1.1 ORGANOPHOSPHATE ESTERS IN THE ENVIRONMENT.

In biological systems, organophosphate esters that act as nerve agents have been found to reversibly bind to and inactivate the enzyme acetylcholinesterase (AChE), inhibiting the breakdown of acetylcholine and leading to an excess of acetylcholine in cholinergic synapses. This excess acetylcholine initially over stimulates and then paralyses cholinergic transmission. The bond between the nerve agent and AChE becomes irreversible after a period of approximately 24 to 72 hours, a process referred to as aging [9].Toxic organophosphate esters find wide application in the environment in the form of pesticides and insecticides. Some common organophosphate insecticides includes; diazinion, Malathion, parathion, chlorothion, dichlorovos [10] and so many others. More harmful chemicals in the same group include chemical warfare nerve agents. They are termed nerve agents (neurotoxins) because they cause cumulative damage to the nervous system and the liver. Nerve agents are easily absorbed by the victim through inhalation, skin contact, or mucosal absorption. Some known organophosphate nerve agents are listed below;

(a) Tabun (O-ethyl N, N-dimethylphosphoroamidocyanidate) otherwise known as GA which is easily produced and its precursor chemicals available.
(b) Sarin (O-isopropyl methylphosphonofluoridate), also known as GB, a colorless, odorless and tasteless liquid in its purest form.
(c) Soman (O-pinacolylmethylphosphonofluoridate) known as GD, which has a slight camphor smell.
(d) GF, this is among the class labeled the G-series and has no common name.

(e) VX (O-ethyl S-2-diisopropylaminoethylmethylphosphonothiolate), a colorless, odorless oily liquid which can be absorbed easily through the skin and by inhalation also.
(f) VR (O-isobutyl S-[2-diethylaminoethyl] methylthiophosphonate) otherwise called Russian VX.
(g) VE, VG, VM, VX and GV are all group of agents known as the 'V series' and the more recent 'GV' series combines severe harmful properties of the other group, posing a threat through inhalation or contact absorption [11].

The term nerve gas is a misnomer as most of these compounds are predominantly liquid at room temperature. They only pose inhalation threats when used as aerosols [12].
Organophosphate containing pesticides are the most widely used type of pesticide. Despite their potential environmental problems, the use of organophosphate pesticides has been increasing and is predicted to increase in the future due to lack of suitable substitutes. Long lived pesticides pose a threat when they spread beyond their intended applications [13-14]. Below is a table that shows toxicity level of some common nerve agents [11].

Table 1.0 Estimated measure of toxicity of some common nerve agents.

	LD_{50}(percutaneous)	LC_{50}	LC_{t50}	IDLH
Tabun(GA)	1gm/person	2ppm	100-400mg x min.	0.03ppm
Sarin(GB)	1.7gm/person	1.2ppm	50-100mg x min.	0.03ppm
Soman(GD)	0.35gm/person	0.9ppm	25-70mg x min.	0.008ppm
GF	0.03gm/person	Unknown	Unknown	Unknown
VX	0.01gm/person	0.3ppm	5-50mg x min	0.002ppm

Toxicity is usually measured in terms of a factor known as LD_{50}, which is the average minimum dosage, in milligrams per kilogram of body weight required to kill 50% of a group of a particular species. Toxicity has also been registered in terms of LD_{50} via skin (percutaneous) absorption per individual species and also in terms of a factor known as

LC_{t50}, which is the lethal concentration in milligram-minute per cubic meter required to kill 50% of specie either by inhalation or percutaneous absorption. LC_{t50} stands for concentration- time product that is lethal to 50% of those exposed and reflects toxicity by the inhalational route, while IDLH is the concentration of toxin in air that is immediately dangerous to life and health. For VX vapour in air, two part per billion (2 ppb) is likely to result in toxicity [11].

Toxicity can be understood as a degree of harmful persistence. Some of these chemicals are regarded as safe due to fast degradation. However, environmental rates for their degradation vary as a function of microbial composition of the soil, the type of the contaminant, pH and the availability of sunlight. Tests conducted for the degradation of these compounds under laboratory conditions (pH of 7 and at $25^{o}C$) reveal that biodegradation is about one order of magnitude faster than chemical hydrolysis, which on other hand is ten times faster than photolysis. In ground water (pH 6.5), hydrolysis reaction of organophosphates was found to have a half life of one year and this is found to be ten days under laboratory conditions [15]. This shows organophosphates persist in the environment for a longer period of time. Persistency described as a measure of these harmful chemicals stability under ambient environmental conditions.

The rate of hydrolysis of some selected group of organophosphate esters are shown below [16];

Organophosphate esters	**Rate of hydrolysis ($K_{OH}M^{-1}Sec^{-1}$)**
Carboxylic esters	1.5×10^{-1}
Amides	5.0×10^{-6}
Phosphate esters	6.8×10^{-12}

The prevalence of these toxic chemicals in the environment has been attributed to human activities even as they pose serious threats as environmental pollutants. These activities include:

(a) Unsupervised management of stockpile of expired pesticides.
(b) Improper domestic and agricultural applications of pesticides.
(c) Various uses as chemical warfare nerve agents in terrorist attacks or in combat war situations.

Earlier studies showed that toxic organophosphate chemical agents have been deployed in war situations over a period of time [17]. Table 1.2 shows countries (sites), warfare agents, dates and amount (quantities) that have been successfully destroyed in the previous years.

Table 1.1 Notable chemical warfare agent destruction sites and dates.

Country (site)	**Chemical agent**	**Amount(tonnes)**	**Date**
Rocky mountain arsenal, USA	H	2786	1969-1974
Rocky mountain arsenal, USA	GB	3799	1973-1976
Tooele (CAMDS), USA	GB	34.5	1981-1986
JACAD Johnston Atoll USA-OVT data	GB	36	1991
Tooele (CAMDS), USA	VX	7	1984
JACAD Johnston Atoll USA-OVT data	VX	49	1992
JACAD Johnston Atoll USA-OVT data	HD	51	1992
DRES, Canada	H	700	1974-1976
DRES, Canada	H	12	1990-1991
DRES, Canada	VX,GA,GB	0.3	1990-1991
DRES, Canada	L	1.5	Not available
Munster, Germany	H	70/year	1980-

Shikhary, Russia	GB, GD, H	300	1980-1990
Shikhary, Russia	VR(Russian VX)	30	1980-1990
Porton Down, UK	H	20	1970
Nancekuke, UK	GB	20	1967-1968
Runcorn, UK	H	6000	1958-1960
Iraq (UNSCOM supervised)	H	500	1992-1993
Iraq (UNSCOM supervised)	GA	30	1992-1993
Iraq (UNSCOM supervised)	GA, GB/GF	70	1992-1993

NOTE: US figures in short tons (2000Ib) converted to tonnes (1000kg). CAMDS was a chemical agent munitions disposal system experimental facility at the Tooele army depot in Utah. This JACADS data is OVT (operation verification test) data obtained prior the full scale operation of the Johnston Atoll chemical agent disposal system. [17]

Although the efforts devoted in researching for effective means of destroying these toxic chemicals is valued, emphasis should be laid on the countries that lack the finances, technologies and expertise of their advanced counterparts in battling the same plague that scourges their daily living. Most of these harmful chemical are dumped in the land and waters of the developing countries and they are made to believe that these compounds are entirely safe and free from potential harm.

Slotkin and Seidler [18] have reported comparative developmental neurotoxicity of organophosphates in vivo. They studied the effects of organophosphates in brain cell development, cell signaling and possible inhibition of neuro-transmitter system in mammals. Lower animals like fowl, cats, dogs and rats have been used to test toxicity of phosphate esters and these chemicals were found to depress plasma cholinesterase in their victims as investigated in the literatures [19]. It has also been reported that the fresh water invertebrates and fishes experiences acute toxicity which results in feeding reduction, discoloration of tissue and finally death. This has been documented by Nevins and Johnson in their experiment with phosphate esters and fish samples to measure toxicity [20].

Much research consideration has been directed towards reducing the environmental problems caused by the presence of organophosphate esters that are toxic and can accumulate in the biosphere and organisms. In the past, dilution was used as a solution to these pollution problems, but due to the fact that pollution levels in our rural and urban environment have increased so much in amount and toxicity, this approach is no longer acceptable. The most versatile decontamination method commonly used is washing and spraying with water that contains soap or detergents. The disadvantage of this method is that, although most of the contaminants are diluted and removed, not all of them are neutralized or destroyed. To neutralize and destroy these contaminants, the addition of bleach (i.e. hypochlorite or other active chlorine containing compounds in alkaline aqueous solution (pH ~ 11) is utilized, which on its own poses problems associated with chlorination.

Several techniques have been developed and utilized over the years to address pollution threats posed by the presence of these toxic organophosphates esters in the environment. Some of the techniques are [17];

(a) Nuclear incineration.
(b) Plasma arc process.
(c) Gamma irradiation.
(d) Wet air oxidation.
(e) Molten salt oxidation.
(f) Neutralization processes (especially with NaOH).
(g) Hypochlorite formulations.

However, these known methods have limiting factors such as high cost, flammability problems, excessive heat release, effluent increase, management problems, and lack of man-power expertise to mention but a few. Bleach for example produces high excessive residues and it is corrosive to surfaces. Incineration is a high tech procedure. Base hydrolysis require large amount of the base to maintain a high pH. Some chemical nerve agents like VX have low solubility in alkaline solutions and so the rate of decomposition is obviously slow [21]. The search for alternatives and more effective decontamination

method still continues. Most important among these various search is the role metal ions play in dephosphorylation reaction involving organophosphate esters.

1.2 METAL IONS IN DEPHOSPHORYLATION REACTIONS

Metal ion containing enzymes or metalloenzymes have been of interest in phosphate esters decontamination studies. Their efficiency in the hydrolysis of polyphosphates and phosphate esters have been widely reported [5-8, 22]. Most organophosphate esters used as toxic nerve agents and pesticides possess a P-O-C linkage in their structure. Cleaving the P-O-C bond could be a means of deactivating these toxic agents. This is convenient due to the nucleophilicity of the phosphorus and the polar nature of P-O and C-O bonds. Metallohydrolases that contain dinuclear active sites are involved in the degradation of agricultural neurotoxins, urea, β-lactam containing antibiotics and several chemical weapons that contain phosphorus (V) compounds [23]. Metal ion containing enzymes are capable of cleaving or hydrolyzing phosphate ester bonds. In essence, enzymes appear to fully utilize the catalytic potential of metal ions [24]. The decontamination of organophosphate ester using metal ions now constitutes a challenging problem which involves phosphoryl transfer reactions.

Enzyme-catalyzed phosphoryl transfer reactions of organophosphate esters and related substances involve the participation of metal ions in almost all cases. The role played by metal ions and metal complexes in facilitating the reactions of phosphate derivatives are given below [25];

(a) Electrophilic activation of the phosphorus centre: A metal ion bonded to the phosphate draws electron away from the phosphorus center. This increases the positive character of the phosphorus centre enabling nucleophilic attack by the nucleophiles in the system thereby cleaving the P-O linkage.

(b) Charge neutralization or Shielding: Phosphate derivatives usually carry many negative charges so the approach of a negatively charged nucleophile such as a hydroxide

ion is not favoured on electrostatic grounds, so the neutralization or shielding of these negative charges is very necessary for a nucleophilic attack at the phosphorous centre.

(c) Orientation of the substrate for hydrolytic attack: Metal ion enhances the optimal stereochemical orientation for intramolecular hydrolytic attack by the nucleophile. The bidentate coordination also results in the formation of a strained chelate activating the substrate for nucleophilic attack as shown below.

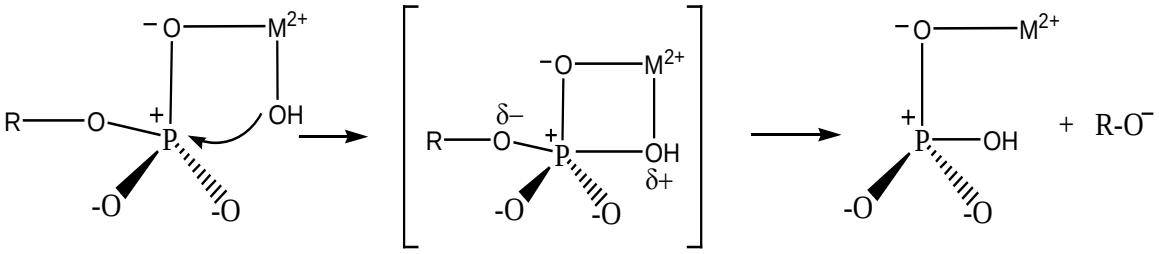

(d) Provision of an effective nucleophile at biological pH: Hydroxide is a better nucleophile than water but its concentration would be low at pH 7.0. Simultaneous coordination of water and phosphate ester to a metal atom overcomes this problem [25]. This is achieved because the conjugate base, hydroxide or alkoxide dissipates its charge through a binding interaction with the metal ion. Since these conjugate bases are better nucleophiles than their parent acids, attack on the electrophilic P atom is enhanced relative to the uncatalyzed reaction. Aqueous coordinated metal ions exist as the following species in solution.

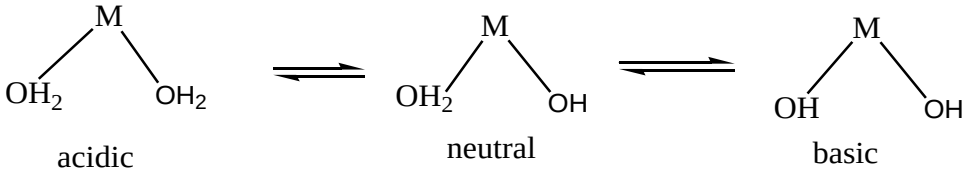

(e) Strain induction: the bidentate coordination of a phosphate to a metal ion could result in the formation of a strained chelate ring thus facilitating a neucleophilic attack at the

phosphorus centre as depicted below.

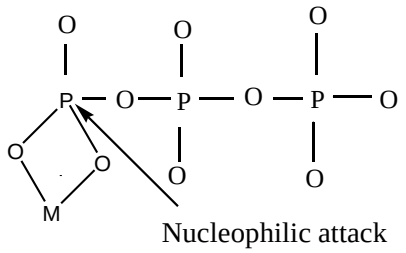

1.2.1 MECHANISM OF PHOSPHORYL TRANSFERS

The mechanism involved in organophosphate esters phosphoryl transfers are formulated as follows [26-28];

(1) Dissociative mechanism: This is otherwise known as the D mechanism (S_N1). It proceeds via an extremely reactive three coordinate metaphosphate intermediate. The nascent trigonal metaphosphate specie could, if free, react with a nucleophile on either face to give a racemic product. The monomeric metaphosphate anion has also been directly observed in the gas phase by mass spectrometry [26].

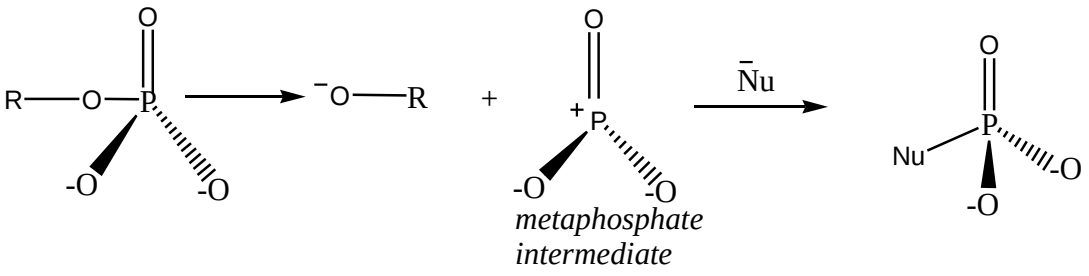

(2) Associative mechanism: This is called the A mechanism (S_N2) and would give an inversion of configuration. It proceeds by the addition of a nucleophile at the phosphorus to generate a five coordinate intermediate or transition state because the phosphorus atom can readily expand its coordination number by use of its d-orbital. An attacking nucleophile such as hydroxide adds to four coordinate phosphorus molecule to give a pentacoordinate phosphorane. Normally the phosphorane will have a trigonal bipyramidal

stereochemistry, but spirocyclic phosphoranes appear to favor square pyramidal structures [27].

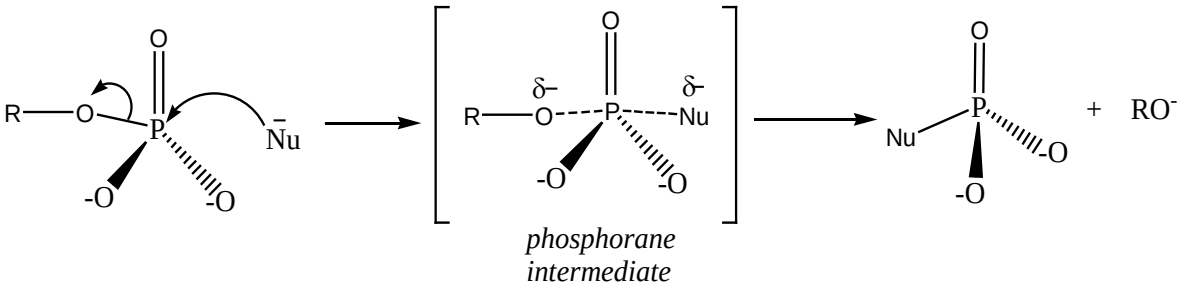

phosphorane intermediate

The associative mechanism can be further explained using the inline addition and the adjacent addition mechanisms but in all a phosphorane intermediate is formed. Both methods only sheds light on the state of the intermediate as displacement and rearrangement within the molecule is achieved.

In-Line Associative Addition: This process gives rise to a pentacoordinate stable intermediate with fully formed bonds. The displacement occurs with inversion of configuration as with S_N2 mechanism.

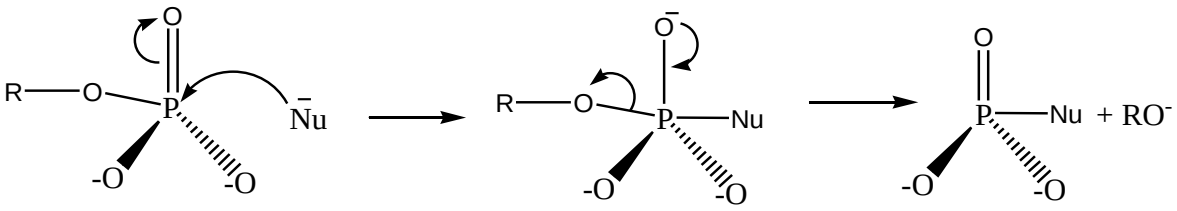

Adjacent Associative Addition-Displacement: This mechanism gives rise to retention of configuration via an adjacent associative mechanism. The pentacoordinate stable intermediate must pseudo-rotate (swap ligands about the P atom between apical and equatorial positions) so that the nucleophile leaves from the apical position.

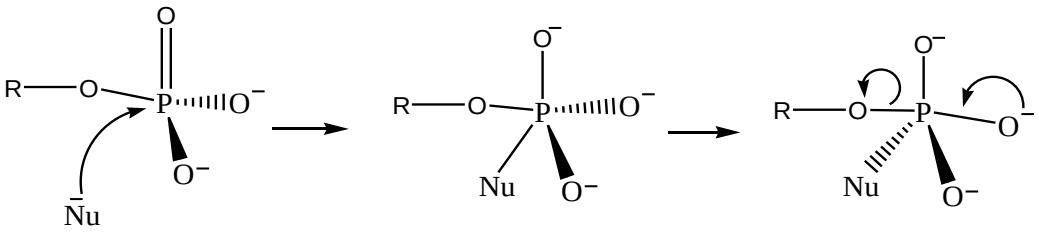

(3) The third type of mechanism is the interchange mechanism otherwise called I mechanism or concerted mechanism. They can be either the I_a type (interchange associative) or the I_d type (interchange dissociative). Interchange mechanisms are characterized by the interchange of ligands X and Y between inner and outer coordination spheres of the metal. When the replacement rate of an outgoing ligand depends on the nature and concentration of the entering ligand, the associative and the I_a mechanisms are possible. If the replacement rate is independent of the nature of the entering ligand, then the mechanism is dissociative or I_d.

The D and I_d mechanisms are difficult to distinguish because the differences depend on the energy well of the intermediate. If the intermediate is relatively stable and lives long enough (on the scale probably longer than 10^{-10}s), to be able to distinguish the entering ligand, it will react with the ligands at different rates. This is a condition for D mechanism. Thus, if two entering ligands Y' and Y" are present (competitive reactions), the products will not be formed statistically (e.g. 50% MY' and 50% MY"), but one of the products will predominate which strongly indicates that the D mechanism is operative. On the other hand, if the intermediate is exceedingly short lived (shorter than 10^{-10}s); it cannot discriminate between the entering ligands. The free coordination position is then occupied statistically, namely according to entering ligands' concentration. This is so called 'accidental bimolecularity'. Here the reaction rate depends on the entering ligands concentration and not on its nature (this statement disregards the ligands salvation effect, steric effects and electric dipole charges effects, which usually ought not to be neglected). The leaving ligand X leaves the coordination shell and enters the solvation shell. The return from the solvation shell into the coordination shell is possible, but not if the entering ligand is in great excess and dominates the solvation shell. This is commonly the case because replacements are

usually carried out under pseudo-first order conditions. (E.g. Y is in 10 to 100 fold excess over X). In such an I_d process, the reaction rate depends on the entering ligand concentration, but not on its nature [28]. Phosphate di- and tri-esters react exclusively via the associative mechanism. Phosphate monoesters however, can react by both associative and dissociative mechanisms depending on their state of protonation [29]. But the neutral esters $(HO)_2PO(OR)$ always appear to react by the associative pathway.

Apart from metal ion catalysis in phosphoryl transfer, the less specific enzymes (alkaline and acid phosphatases) operate via phosphorylated enzyme intermediates. Bimetallic and polymetallic centers have been used as catalytic sites in many phosphoryl and nucleotydyl transfer reactions studies [25] of enzymes with Zn (II) – Zn (II) active sites that include phosphoprotein phosphatases, alkaline phosphatases and phosphotriesterases. The common occurrence of bimetallic/polymetallic active centre is rationalized by the two metal ion mechanism where presumably both the general Lewis acid properties and charge effects are considered. Two metal ion mechanism is operative with the main group metal ions as corroborated by the fact that both Zn^{2+} and Mg^{2+} are common in these hydrolytic enzymes (alkaline phosphatases, yeast inorganic pyrophosphatases, kinases and purple acid phosphatases). An overview of these phosphatase enzymes is given below.

1.3 PHOSPHATASE ENZYMES

Phosphotases are groups of enzymes that remove a phosphate group from its substrate by hydrolyzing phosphoric acid monoesters into a phosphate ion and a molecule with a free hydroxyl group. This action is directly opposite to that of phosphorylases and kinases, which attach phosphate groups to their substrates by using energetic molecules like ATP [30]. Phosphatases can be categorized into two main categories namely;

(a) Cysteine dependent phosphatases: These phosphatases catalyses the hydrolysis of a phosphate ester bond giving rise to a phospho-cysteine intermediate [31]. They do so by forming a bond with the phosphorus atom of the phosphate moiety protonating the P-O

bond linking the phosphate group to the substrate. The phospho-cysteine intermediate is then hydrolyzed by a water molecule, thus generating the active site for another dephosphorylation reaction.

(b) Metalophosphatases: These phosphotases are dependent on metal ions in their active sites for activity. They coordinate two catalytically essential metal ions within their active site with a hydroxyl ion bridging the two metal ions. This bridging ion takes part in nucleophilic attack on the phosphorus ion [30]. A common phosphatase in many organisms is the alkaline phosphatase.

1.3.1 ALKALINE PHOSPHATASE

Alkaline phosphatase is a non specific phosphomonoesterase which shows maximum activity at pH 9-10. The enzyme from E.Coli is a dimer with molecular weight (Mr) of 94000. It contains at least two to four Zn^{2+} ions and Mg^{2+} ions per dimer. It consists of 449 amino acid residue subunits and contains two active sites. Each active site binds to two Zn^{2+} ions and one Mg^{2+} ion. The metal ions appear to play two roles in the enzymatic reaction. Two Zn^{2+} ions are required for activity and are bound strongly to the enzyme, playing catalytic role. The other two Zn^{2+} ions and the Mg^{2+} ion stabilize its tertiary and quaternary structure thereby enhancing the activity of the enzyme. Although much is known about the reaction of the active site, the role of the metal ion in the reaction mechanism is still unclear and the degree of involvement of other functional groups surrounding this hydrolyzing enzyme is yet to be established [32].

1.3.2 ACID PHOSPHATASE

Very less is known about acid phosphatases, a family of non-specific enzymes of molecular weight (Mr) 40000-60000. The enzymes have been isolated from a variety of sources including yeast, human lysosomes and human prostate as well as plants and bacteria. These enzymes have an optimum pH of 2.5 and do not require metal ion cofactors for catalysis [33]. The enzyme from different sources show limited amino acid sequence homology, although certain regions of the protein are highly conserved, in

particular, a motif near the N-terminal which includes Arg-His-Gly-Xaa-Arg-Yaa-Pro (positions 16-22 in the E.Coli enzyme)[34]. The enzyme displays many characteristics indicative of a ping-pong phosphorylated enzyme intermediate mechanism. [35-36]. The stereo chemical course of the transphosphorylation reaction catalyzed by the enzyme and determined in an analogous manner to that of alkaline phosphatase shows retention of configuration for the two transfer steps. Again there is no documented result yet showing conclusive evidence on the stereo chemical course of the individual transfer steps.

1.3.3 YEAST INORGANIC PYROPHOSPHATASE

This enzyme consists of two identical subunits with a molecular weight (Mr) of 64000 for the dimer. It functions as a catalyst in the reversible hydrolysis of pyrophosphates. In the presence of Mg^{2+} yeast inorganic pyrophosphatase catalyzes pyrophosphates specifically. However it becomes less specific and hydrolyses a number of pyrophosphate esters in the presence of other metals [37]. Ba^{2+} and Ca^{2+} ions inhibit the enzyme activities while Mg^{2+}, Mn^{2+}, Co^{2+}, Zn^{2+}, Ni^{2+}, Fe^{2+} and Cd activate it [38]. It has been shown conclusively that one metal ion is required to form the substrate and at least one divalent ion is required for activity [39-41]. The basic mechanism for yeast inorganic pyrophosphatase reaction includes: metal ion binding to the pyrophosphate to produce a substrate, production of a metal bound hydroxo-ligand as a nucleophile by an adjacent basic amino acid residue and stabilization of substrate by interaction with cationic amino acid residue [42, 43].

1.3.4 PURPLE ACID PHOSPHATASE

These are metalloenzymes that hydrolyze phosphate esters and anhydrides under low pH [44]. In their oxidized form, purple acid phosphatases in solution are purple in colour as a result of charge transfer. This is due to the presence of a dinuclear iron centre [45] to which a tyrosine residue is connected [46]. The metallic centre is composed of $Fe^{3+}$and M, where M is Fe^{3+}, Zn^{2+}, Mg^{2+} or Mn^{2+}. The oxidized form contains two antiferromagnetically coupled Fe^{3+} ions, which is purple in color and inactive to

phosphate ester hydrolysis [32]. Reduction from Fe^{3+} to Fe^{2+} makes it active to hydrolytic functions and the color turns to pink. Treatments with strong reducing agents dissociate the metallic ions and render the enzyme colorless and inactive [47]. The metallic nucleus of PAPs varies between plants and mammals. Mammalian PAPs which have been isolated and purified are composed of iron ions, whereas in plants the metallic nucleus is composed of Fe^{3+} and either Zn^{2+} or $Mn^{2+.}$ They have also been isolated in fungi and DNA sequences. PAPs have also been identified in prokaryotic organisms such as cyanobacteria species and mycobacteria species. A descriptive mechanism for PAP hydrolysis of a phosphomonoester is shown in the scheme below [48].

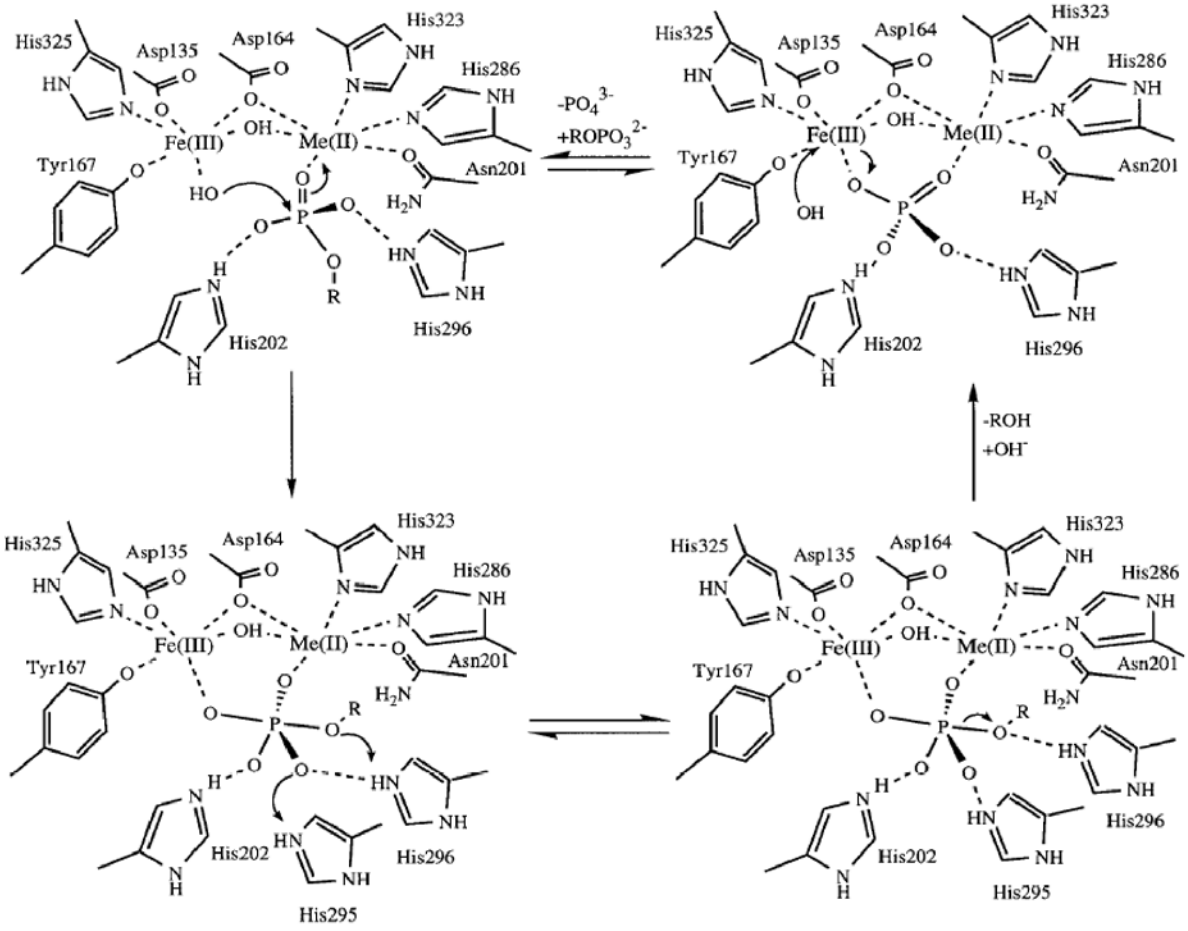

Scheme 1.0 Tentative mechanism of a phosphomonoester hydrolysis by PAP.

(The pentacordinate transition state is presumed to be stabilized by the metal ions (His 202 and His 296). The release of the alcohol component under inversion of the configuration at the phosphorus is presumably promoted by the protonation by the His 296. The release of the phosphate group requires attack of the water molecule at Fe (III) in other to start another cycle of catalysis)

1.3.5 PROTEIN PHOSPHATASE

These are a diverse group of enzymes responsible for the dephosphorylation of a range of phosphoproteins. Many are involved in the regulatory control of cellular processes as diverse as cell growth and proliferation, protein biosynthesis, cholesterol and fatty acid biosynthesis and glycolysis/gluconeogenesis. The protein phosphatases can be categorized into two large groups; those that dephosphorylate phosphotyrosine residues within protein and those that dephosphorylate phosphoserine or phosphothreonine residues within proteins.

1.3.6 NUCLEOTIDASE

Nucleotidases are hydrolytic enzymes that catalyze the hydrolysis of a nucleotide into a nucleoside and a phosphate. Good examples are the conversion of adenosine monophosphate to adenosine and guanosine monophosphate to guanosine. They break down nucleic acid on digestion. They are categorized into two based on the end which is hydrolyzed; we have the 5'nucleotidases and the 3'nucleotidase. 5' nucleotidases cleave off the phosphate from the 5'end of the sugar moiety. They are involved in varied functions like cell-cell communication, nucleic acid repair, purine salvage (pathway for the synthesis of nucleotides); signal transduction, membrane transport etc. 5'nucleotidase activity was first discovered in the venom of snakes and has since been isolated from a wide variety of species including bacteria, plants and mammals [49].

1.3.7 INOSITOL MONOPHOSPHATASE

These catalyze the hydrolysis of both enantiomers of myo-inositol 1-phosphates, myo-inositol 4-phosphates and a range of nucleoside 2'-phosphates. This enzyme is believed to be an important target for lithium therapy in the treatment of maniac depression [50]. The enzyme is inhibited by Li^+ in the millimolar concentration range as used in therapy and is even more sensitive to Li^+ at the physiological concentrations of the inorganic phosphate present in the brain (2-5mM). They have been purified to homogeneity from a

number of mammalian sources such as rats, bovine and human brain. They show absolute requirement for a divalent metal ion and activity is supported by Mg^{2+}, Mn^{2+}, and Zn^{2+} ions [51, 52].

1.3.8 KINASE

A kinase alternatively known as a phosphotranferase is a type of enzyme that transfers phosphate groups from high energy donor molecules such as ATP to a specific target molecule (substrates). This process is known as phosphorylation. Kinases require at least one divalent metal ion (usually Mg^{2+}) for activity. One of the largest groups of kinase is protein kinase, which act on and modify the activity of specific enzymes.
The overall catalyzed reaction of nucleoside 5'-triphosphate to nucleoside 5'-diphosphate is a typical kinase reaction and can be depicted as [53, 54];

1.4 AIM OF THE STUDY

Most of the enzyme systems described above require metal ions for activity. Some invariably, effect dephosphorylation of phosphate esters in the absence of a metal cofactor. Our research emulates nature's definitive process of phosphate ester decontamination. We tend to replicate the activities of these biological enzymes in vitro using model systems involving metals and non-metals. This can be achieved by drawing inspiration from the structures, compositions and mode of operation of these specific enzymes. Armed with this vision, we set out to achieve the following;

(a) To study the dephosphorylation of phosphate esters using 4- nitrophenylphosphate as an activated phosphate model and sodium pyrophosphate as an un-activated substrate model for organophosphates.

(b) To investigate the effects of bis(trimethylenediamine) hydroxoaquocobalt(III) ion $[Co(tn)_2(OH)(H_2O)]^{2+}$ as an enzyme model.

(c) To investigate the roles played by oxides of nitrogen in dephosphorylation reactions in the biosphere.

(d) To study the synergistic cooperativity between bis(trimethylenediamine) hydroxoaquocobalt(III) ion $[Co(tn)_2(OH)(H_2O)]^{2+}$ complexes and nitric oxide in the dephosphorylation reactions involving phosphate esters

(e) To formulate decontamination solutions which are environmentally friendly, fast, efficient, cheap and effective under ambient conditions.

To achieve our desired goal, the following model systems were utilized in our investigation.

1.4 .1 Co (III) ENZYME MODEL SYSTEM

The following were the reasons why Co(III) complexes were utilized as our enzyme model [55].

(a) Model systems based on Co(III) complexes are especially advantageous in that metal coordination sites open for phosphate substitution can be limited. This permits studies of a type not readily available using labile metal centers.

(b) Co(III) complexes are exchange inert and so its complexes are thermodynamically stable thus making the mechanisms and kinetics of Co(III) complexes to be well understood.

(c) The (-Co-N- bonds) in Co(III) amine and polyamine complexes retain their integrity in aqueous media for a long time.

(d) Co(III) complexes are easy to synthesis and are kinetically robust thereby permitting the characterization of all species present in the solution.

(e) Co(III) is a low spin d^6 ion; it is diamagnetic and therefore enables ^{31}P studies as a probe for monitoring the reactions.

1.4.2 P-NITROPHENYLPHOSPHATE (4-NPP): SUBSTRATE MODEL FOR ACTIVATED PHOSPHATE ESTER

4-Nitrophenylphosphate (4-NPP) produces nitrophenolate ion and a phosphate moiety on dephosphorylation. Rate of this reaction in the pH range of 4 to 9 is both essentially constant and very slow [56]. Under slightly basic condition the p-nitrophenol is deprotonated to form the p-nitrophenolate ion which is bright yellow and has maximum absorbance at 400nm. In an unbuffered solution the acid-base reaction of p-nitrophenol changes in concentration resulting in a shift in the equilibrium position and a consequent deviation from Beer's law. In a buffered solution, the pH would be fixed and the ratio of the concentration of p-nitrophenolate to the p-nitrophenol will be constant thereby obeying to Beer's law.

Calibration studies done using solutions of p-nitrophenol and p-nitrophenylphosphate within a concentration range of 10^{-3}M – 10^{-6}M at 25^{o}C and pH of 7, in a buffered solution, shows that 4-NPP has absorption maximum at 310nm distinct from p-nitrophenolate ion that absorbs at 400nm as shown in figure 1.0. Distinct measurement of p-nitrophenolate production as a result of dephosphorylation can be achieved without interference from the parent 4-NPP. From the calibration curve, the amount of p-nitrophenolate ion can be calculated assuming 100% p-nitrophenolate production for complete hydrolysis [8].

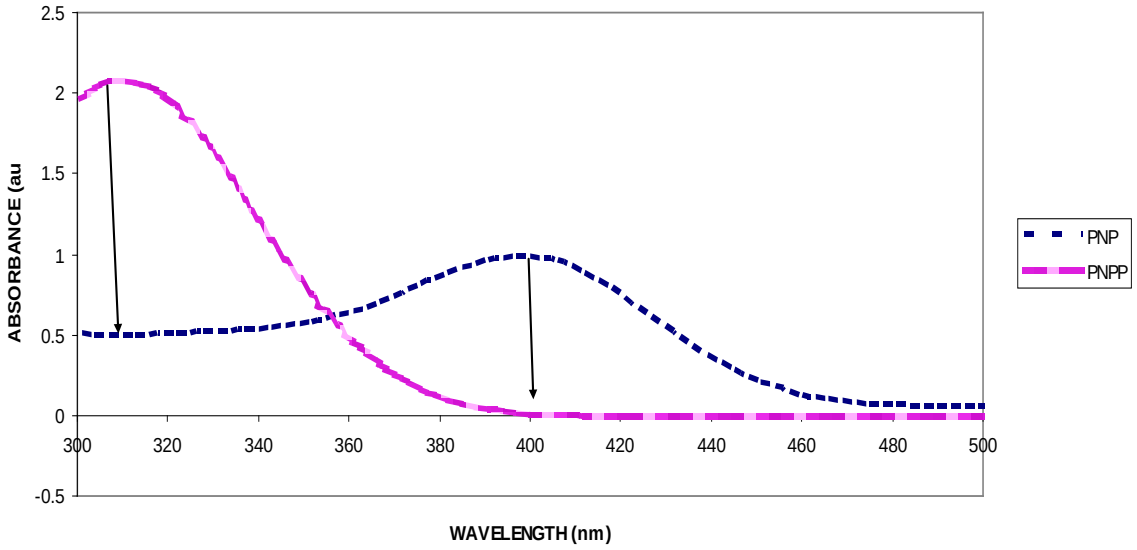

Figure 1.0 Absorption spectra of NPP and NP at 25^{o}C and pH of 7.

1.4.3 SODIUM PYROPHOSPHATE: SUBSTRATE MODEL FOR UNACIVATED PHOSPHATE ESTER

Polyphosphates are essential to life processes and understanding their hydrolysis and related phosphoryl transfer involving cleavage within the P-O-P framework is of paramount importance. In biological systems, these reactions are catalyzed by enzymes which contain metal cations or require them as co-factors. In the absence of enzymic catalysis, hydrolysis reactions of simple polyphosphates such as pyrophosphate, linear triphosphate, adenosine-diphosphate and adenosine-triphosphate normally proceed extremely slowly in all but highly acidic media [57].

It is known that the hydrolysis of free pyrophosphate at constant pH follows pseudo-first order kinetics [58]. Catalytic effects of metal ions on the hydrolysis of pyrophosphate have been widely reported and the effect of pH, ionic strength and temperature are well documented [59-60]. Earlier studies [57] done in this area showed that in the presence of an excess bis(trimethylenediamine) hydroxoaquacobalt(III) ion $[Co(tn)_2(OH)(H_2O)]^{2+}$, the degradation process is relatively rapid at 25^{o}C and pH 7 for a 3:1 Co to PPi ratio at

10^{-2} molar concentration. Literature studies [61] have reported even greater rate of cleavage under the same conditions using $[Co(tn)_2(OH)(H_2O)]^{2+}$ with preformed $[Co(en)_2HP_2O_7]$. These studies were based on ^{31}P NMR analysis of quenched reaction aliquots where the cobalt(III) complex was decomposed and $PO_4^{3-}/P_2O_7^{4-}$ were determined from the peak areas of their signals. In the former study, the pyrophosphate complex was quenched with sodium hydroxide (0.5M OH^- in the final solution) for a period of three days [57], while the later study utilized quenching with cyanide [61]. In this particular study, 4-nitrophenylphosphate is modeled as an activated phosphate model while the sodium pyrophosphate acts as an unactivated substrate phosphate model. Another interesting choice for an enzyme model is the nitric oxide compound. A brief description and reasons for choosing the radical is briefly explained below.

1.4.4 CHOICE OF NITRIC OXIDE AS A TRIGGER

Nitric oxide is a colorless gas with virtually no water solubility. In the presence of excess oxygen, it slowly converts to nitrogen dioxide. This gas is produced in great quantities in internal combustion engines. The unique features in the properties and reactions of the nitric oxide molecule arise largely from its ability to exist in the three forms NO^+, NO and NO^-. In many reactions the nitric oxide group loses or gains an electron, but otherwise retains its identity. The monomeric nitric oxide group contains an odd electron and its mode of compound formation are; (i) the sharing of an electron pair to give a covalent compound $X^{\cdot}NO$, (ii) the gain of an electron to form the anion NO^- and (iii) the loss of one electron to form the cation NO^+. Since nitric oxide is an odd-electron molecule it might be expected to dimerise readily. The resonance energy stabilizes the monomeric form to such an extent that the heat of dimerization becomes negative. The dimer is only obtained at low temperatures [62].

Nitric oxide is thought as a poisonous gas that causes air pollution and acid rain. It readily converts to NO_2 in air which undergoes dissociation to nitric oxide and oxygen in the presence of sunlight. In the troposphere the readily available NO_2 reacts with hydrocarbon peroxy radicals (RO_2), along with olefins, aldehydes, C_2H_2, CO and

peroxyacylnitrates to form a mixture described as photochemical smog which pollutes the air [63]. It was believed that apart from its threat to human health and the ecology, it has no positive function. Scientific discoveries have greatly increased interest in the nitric oxide molecule. It has been shown that nitric oxide is responsible for several important biological events including vascular smooth muscle relaxation [64], platelet deaggregation [65-66], neuronal communication [67], and possible photoreceptor signaling [68]. The involvement of nitric oxide has been found to occur through the activation of guanylate cyclase, a heme-containing enzyme which catalyzes the reaction of guanosine triphosphate (GTP) to cyclic guanosine monophosphate cGMP)[69]. Nitric oxide released by murine macrophages and other cells after immunological activation act as a cytotoxic molecule for invading intracellular micro-organisms and tumor cells [70]. In all cases, the inhibition of enzyme activity was accompanied by the loss of intracellular iron from the target cells. Also, the enzyme nitric oxide synthase converts L-arginine and yields nitric oxide [71]. The endogenously produced nitric oxide is known as endothelium-derived relaxation factor (EDRF) because of its role in the relaxation of vascular smooth muscles. These and related observations have raised the question, "WHY NITRIC OXIDE?" What makes the compound so special that it is used as a trigger for these important processes? Researchers are now left to wonder what other processes and functions this compound performs. A very important process in nature that involved the release of nitric oxide in biological functions is explained in the photolysis of nitrates and nitrites.

1.4.4.1 PHOTOLYSIS OF NITRATES AND NITRITES

Photo transformation plays an important role in the degradation of organic substances present in natural waters, particularly in the case of poorly biodegradable pollutants. Direct photolysis takes place with substrates absorbing solar light i.e. wavelength longer than about 300nm. In many instances, organic molecules do not absorb sunlight to an appreciable extent and direct photolysis reactions are negligible. In these cases photo degradation can be induced by environmentally occurring compounds such as inorganic ions (e.g. nitrates and nitrites), transition metals (e.g. Fe^{III} salts) and natural organic

molecules containing carbonyl or phenolic groups (e.g. humic substances). These substances produce radical or oxidizing species upon irradiation [72].

The production of hydroxyl radicals as a result of photolysis within the UVA and UVB region can be depicted as:

NO_3^- + *hν* ⟶ $\cdot NO_2$ + $O^{\cdot -}$ *(305-313nm)*.....1

$O^{\cdot -}$ + H^+ ⇌ $\cdot OH$ 2

NO_3^- + *hν* ⟶ NO_2^- + $O(^3P)$ *(305nm)*.....3

Hydroxyl radicals produced can undergo dimerisation while oxygen atoms react with nitrate and nitrite to give reactions that produces N_2O_4, which hydrolyses to nitrates and nitrites as shown below [72].

$\cdot OH$ + $\cdot OH$ ⟶ H_2O_2 4

$O(^3P)$ + NO_3^- ⟶ O_2 + NO_2^- 5

$O(^3P)$ + NO_2^- ⟶ NO_3^- 6

$\cdot NO_2$ + $\cdot NO_2$ ⇌ N_2O_4 7

N_2O_4 + H_2O ⟶ NO_3^- + NO_2^- + $2H^+$.....8

The irradiation of nitrates also results in the isomerisation to peroxynitrite/peroxynitrous acid. This reaction has been conclusively demonstrated to take place at $\lambda < 280$nm. Its occurrence at higher wavelengths is still uncertain [73].

NO_3^- + *hν* ⟶ $ONOO^-$ *(254nm)*..... 9

$ONOO^-$ + H^+ ⇌ HOONO 10

Due to the generation of hydroxyl radicals, the photolysis of nitrate and nitrite can lead to the degradation of organic compounds [72]. This effect can result in decontamination induced by photolytic processes in natural waters, leading to photoinduced degradation of organic pollutants. This depolluting role of nitrate and nitrite photochemistry is however reduced by the competition between natural organic matters, bicarbonate ions and organic pollutants for reaction with hydroxyl [74]. Furthermore, the overall antipollution role can be counterbalanced by the fact that the UV irradiation of solutions containing aromatic compounds and nitrates or nitrites can lead to the formation of mutagens, with larger

effects observed for nitrites irradiation. Interestingly, the irradiation of nitrites yields $^{\cdot}NO$ + $^{\cdot}OH$ as the major reaction pathway, while a minor pathway of uncertain importance yields $^{\cdot}NO_2$ and aquated electrons [72].

$$NO_2^- + h\nu \longrightarrow {}^{\cdot}NO + O^{\cdot -} \quad (355nm) \quad \text{.....11}$$
$$O^{\cdot -} + H^+ \rightleftharpoons {}^{\cdot}OH \quad \text{.....12}$$
$$NO_2^- + h\nu \longrightarrow {}^{\cdot}NO_2 + e^- \quad (aq) \quad \text{.....13}$$

Nitrates reacting with oxygen in the triplet state $O(^3P)$ yield peroxynitrate which ends up giving hydroxyl radical and nitric oxide radical.

$$NO_3^- + O(^3P) \longrightarrow O_2NOO^- \quad (peroxynitrate) \quad \text{.....14}$$
$$O_2NOO^- + H^+ \longrightarrow HOONO_2 \quad \text{.....15}$$
$$HOONO_2 \longrightarrow HNO_2 + O_2 \quad (nitrous\ acid) \quad \text{.....16}$$
$$HNO2 \longrightarrow {}^{\cdot}OH + {}^{\cdot}NO \quad (280nm\text{-}385nm) \quad \text{.....17}$$

Radiation of nitrates and nitrites are photolytic processes that release nitric oxide in the environment at certain wavelengths of UV absorption. In this research work, nitric oxide production in solution was achieved by UV radiation of sodium nitroprusside at different wavelengths of photolysis.

1.4.4.2 THE SODIUM NITROPRUSSIDE ION

Sodium nitroprusside was used as a precursor for nitric oxide. This compound also known as sodium pentacyanonitrosylferrate (II) $Na_2[Fe(CN)_5NO]^{\cdot}2H_2O$ is available commercially in the dihydrated disodium salt. This red solid dissolves in water to give a solution containing the dianion $[Fe(CN)_5NO]^{2-}$; a metal nitrosyl complex which is a reactive agent. In this anion, the iron is octahedral, surrounded by five tightly bond cyanide ligands and one nitric oxide ligand. When the linear nitrosyl ligand is assigned a single positive charge, the iron is assigned the oxidation state of 2+. As such that it has a low spin d^6 electron configuration. This diamagnetic ion is shown in figure 1.1 below [75, 76].

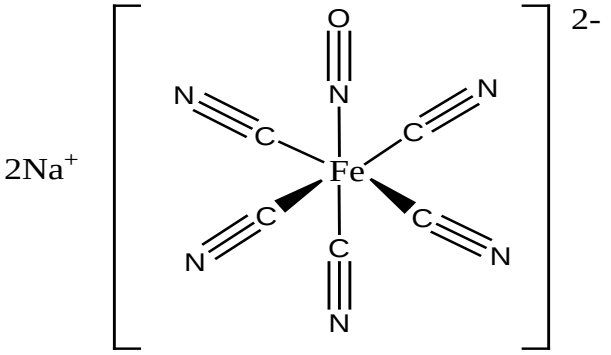

Figure 1.1 The sodium nitroprusside ion

The photosensitivity of SNP has been studied by many authors [75-77]. Part of this interest has been directed towards elucidating the species formed under irradiation [78-79]. A very recent interest in the photosensitivity of this compound is its widespread uses as a potent vasodilator for the lowering of blood pressure during surgery, management of hypertensive crises and cardiac failure [80]. Sodium nitroprusside (often abbreviated SNP) is frequently used in vascular research to test endothelium-independent vasodilation. One method of administering SNP is by iontophoresis. This allows local administration of the drug, causing local microvascular vasodilation. NO liberated from the SNP diffuses into the vascular smooth muscle causing relaxation and subsequent vasodilatation. This vasodilatation is quantified by various techniques. This important role aids in the treatment of hypertension. SNP is also often used as a reference compound for the calibration of Mossbauer spectrometer.

Some authors have reported decomposition of SNP on mixing with blood as cyanide is been released [81]. Bisset and Butler [80] have concluded that it is light and not blood that is responsible for the release of the cyanide. Mitra and Jain [78] studied the pH changes during the photolysis of $[Fe(CN)_5NO]^{2-}$ solutions with unfiltered light. It was observed in another study that there was a larger change in pH of aerated solutions compared with deaerated solutions [82]. They suggests a photo process involving the ejection of NO which can be oxidized to NO_2 and producing NO_2^-, NO_3^- and H_3O^+ ions. Wolfe and Swinehart [83], however ruled out the NO^+ production based on experiments with labeled water and labeled $[Fe(CN)_5NO]^{2-}$ solution. They proposed that the change in hydrogen-ion concentration during photolysis could be partly due to nitric oxide

production, followed by hydrolysis of the aquacyanoferrate(III) species according to the reactions below;

$$[Fe(CN)_5(NO)]^{2-} + H_2O \xrightarrow{h\nu} [Fe^{III}(CN)_5(H_2O)]^{2-} + NO \quad \text{.....18}$$

$$[Fe^{III}(CN)_5(H_2O)]^{2-} \rightleftharpoons [Fe(CN)_5(OH)]^{3-} + H_3O^+ \quad \text{.....19}$$

Espenson and Wolenuk [84] have shown the specie with an absorption maximum at 400nm to be the aquacyanoferrate (III) ion, $[Fe^{III}(CN)_5(H_2O)]^{2-}$. This lends credence to equation (18) above as the primary process in nitroprusside photolysis. Stochel [85] using UV/Vis spectroscopy also found evidence for the loss of nitric oxide in a primary photo substitution process. (solv. = solvent molecule).

$$[Fe(CN)_5(NO)]^{2-} \xrightarrow{h\nu} [Fe^{III}(CN)_5(solv)]^{2-} + NO \quad \text{.....20}$$

The production of HCN and $(CN)_2$ is only noted as a secondary phenomenon in solutions that have a high concentration of $[Fe(CN)_5(NO)]^{2-}$ ($>10^{-2}$M) after an extended period (>3 hours) of photolysis [86]. A brief description of electromagnetic spectrum and UV radiation is given below to elucidate the different wavelengths at which this processes can be obtained.

1.4.4.3 ELECTROMAGNETIC RADIATION

Electromagnetic radiation is usually characterized by wavelength and is expressed in terms of nanometers (10^{-9}m) often abbreviated as nm. Wavelengths have also been commonly measured in terms of millimicrometers or millimicrons (mμ) and earlier in Angstrom units (ǺU).

10 ǺU = 1nm = 1 mμ

The ultraviolet portion of the electromagnetic radiation has been commonly divided into different regions as depicted in figure 1.2 overleaf.

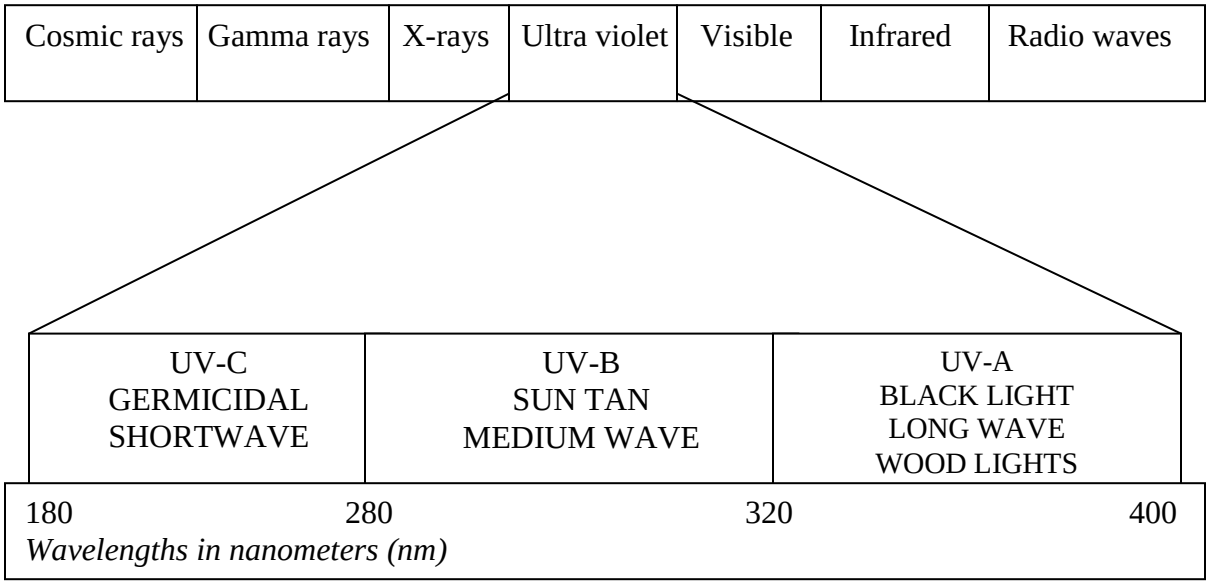

Figure 1.2 The electromagnetic radiation spectrum

(a) THE SHORT WAVELENGTH REGION – Also known as far ultraviolet, germicidal or UV-C, extends from 180nm – 280nm. Although it has little penetrating power, short wave UV causes severe burns to the eyes and skin. When short waves affect the eyes, the discomfort is commonly known as 'welders flash' or 'ground glass eyeball'. The usual artificial sources of this radiation are low pressure mercury vapour lamps (and contain other metal vapour lamps) used in UV sterilization, chromatography, mineralogy, photochemical reactions etc [87].

(b) THE MEDIUM WAVELENGTH REGION- This is also known as middle ultraviolet, erythemal or UV-B and extends from 280nm to 320nm. It has high penetrating power and can seriously burn the eyes and the skin. The usual artificial source of this radiation is sun lamps, used for cosmetic or therapeutic purposes and vitamin production.

(c) THE LONG WAVELENGTH REGION- This region is also called the near ultraviolet, black light, woods light or UV-A and extends from 320nm to 400nm. A portion of the population is overly sensitive to radiation in this region of the spectrum and may experience adverse negative reactions like "blue haze" interference due to the

fluorescent effect of rays from this region in the ocular media. The usual artificial sources of this radiation are low and medium pressure mercury vapour lamps used in non destructive testing, quality control inspection, leak detection, medical diagnosis, and UV curing and general fluorescence analysis [87].

Ultraviolet radiations are emitted naturally in sunlight or by electric arcs and specialized lights such as black lights. It is an ionizing radiation and induces chemical reactions in humans and the ecology. Most natural reactions, like the human production of vitamin D is as a result of the exposure of the skin to UV-B. Vitamin D deficiency in human causes bone diseases attributed to bad absorption of calcium. Too much UV-B also leads to DNA damage, cancer and sunburn. Obviously the interaction of UV radiation with the environment leads to chemical changes which affect the environment. In this particular study, our interest lies in the interactive mode of natural UV radiation with naturally occurring compounds like nitrates and nitrite which gives rise to nucleophilic radicals that can effect dephosphorylation in the biosphere. Our experiments are designed to replicate natural phenomena like UV radiations in vitro and attempt dephosphorylation of organophosphate esters under prevalent environmental conditions. This is incorporated in our method of analysis and instrumentation to be discussed in the experimental section.

CHAPTER TWO

2.0 EXPERIMENTAL

2.1 INSTRUMENTS AND REAGENTS

All reagents used were either analytical reagent grade or the purest available commercially and were used without further purification. Measurement of pH was made with Metrohm 632-pH meter with a combination electrode. Cecil Aquarius CE9200V and thermospectronic Genesys 2 UV/Vis spectrometers were used to obtain spectra while a Genesys 10 UV/Vis spectrometer was used to collect rate data. A modified spectroline model CX-21 ultraviolet fluorescence cabinet with long wave UV (365nm), short wave UV (254nm) and white light was utilized as photolysing chamber. The long wave UV source provides a typical peak intensity of 610μW/cm^2, while the short wave source has an intensity of 500μW/cm^2. The pH of the reaction mixture was maintained by adding drops of 0.1M, 0.01M and 0.001M solutions of NaOH or $HClO_4$ using different marked dotting glass rods in a simple technique referred to as glass stick dotting. The diaqua complex $[Co(tn)_2(H_2O)_2]^{3+}$ was prepared in solution from the carbonato complex $[Co(tn)_2(CO_3)]$ as will be described later. The temperature of the reaction was controlled using a thermostated water bath which allows the constant temperature water to circulate via a jacketed reaction vessel as shown in figure 2.0.

Figure 2.0 Experimental set up

(As a precaution, all model compounds used in the experiments were prepared and used the same day, as its chemical composition deteriorates upon standing)

2.2 SYNTHESIS OF SODIUM TRIS-CARBONATOCOBALTATE(III) TRIHYDRATE ($Na_3[Co(CO_3)_3].3H_2O$)

The method developed by Bauer and Drinkard [88] was utilised. Sodium tris-carbonatocobaltate(III) trihydrate $Na_3[Co(CO_3)_3].3H_2O$ was synthesized and utilized as a precursor for the preparation of a representative group of cobalt(III) compounds as it possesses the following advantages:

(a) The acidic form of the ligand may be used. This is preferred over the basic ligand that aids oxidation and absorption of carbondioxide from the surroundings, thus increasing volatility problems.

(b) The compound is very stable on storage, if kept dry and away from UV rays. It is

also very reactive under mild conditions.

(c) The general preparation of this compound is not tedious or time consuming and the starting materials are readily available.

(d) Since the acidic form of the ligand can be used, the evolution of carbondioxide gas presumably drives the reaction to completion even under mild conditions.

The following method of synthesis was adopted for the preparation of the Sodium tris-carbonatocobaltate(III) trihydrate $Na_3[Co(CO_3)_3].3H_20$ complex. The purity of the compound was verified by comparing its electronic spectra with that reported in the literature [89].

A 50mL solution of 29.1g of $Co(NO_3)_2.6H_2O$ (0.1 mole) and 10mL of 30% hydrogen peroxide (excess) was added drop wise with stirring to a cold slurry of 42.0g of sodium bicarbonate (0.5 mole) in 50mL of H_2O. The mixture was allowed to stand at 0^oC for 1 hour with continuous stirring. The olive product was filtered, washed on the filter with three 10mL portions of ice cold water, and then thoroughly washed with absolute ethanol and dry ether. The yield was 39.12g and the percentage yield was calculated as 94.23%.
It is important to mention that the number of base equivalents per mole of intermediate is six. Thus, the number of coordination positions per mole is equal to the number of base equivalents per mole.

2.2.1 CONVERSION OF SODIUM TRIS-CARBONATOCOBALTATE(III) TRIHYDRATE ($Na_3[Co(CO_3)_3].3H_2O$) TO CARBONATO BIS ETHYLENEDIAMINE COBALT (III) PERCHLORATE ($[Co(tn)_2CO_3]ClO_4.H_2O$)

A slurry of 3.6g of $Na_3[Co(CO_3)_3].3H_2O$ (0.01 mole) was mixed with 0.02 mole of 1,3 diaminopropane and 0.04 mole of perchloric acid and warmed in a steam bath for two hours. The mole ratio of the intermediate to ligand ($Na_3[Co(CO_3)_3].3H_2O$: ligand) was 1:2 where ligand = bidentate ligand 1,3diaminopropane. The reagent mixture was then filtered hot and the filtrate was saturated with absolute ethanol to precipitate an orange product, which is further recrystallized by placing it in the refrigerator for about 12 hours in an ethanol-water solution. It was observed that a pronounced improvement in both the

quantity and quality of the yield was prominent when the reagents mixture was filtered hot and the filtrate reduced to about one-third of its original volume using rotavapour. After which further precipitation and recrystallization was carried out. The yield recorded was 3.28g which was 87.46% of theoretical expected yield. It was dried in air and converted to the diaquo complex.

2.2.2 CONVERSION OF THE CARBONATO ($[Co(tn)_2CO_3]ClO_4.H_2O$) TO DIAQUO COMPLEX ($[Co(tn)_2(OH_2)_2]^{3+}$)

The conversion of the carbonato ($[Co(tn)_2CO_3]ClO_4.H_2O$) to the diaquo $[Co(tn)_2(OH_2)_2]^{3+}$ complex was achieved by adding 2.5mmol of 6M perchloric acid to 1 mmol of finely divided carbonato specie. The solution was stirred in the dark under a vacuum aspirator for 30 minutes at 50°C. The pH was then adjusted to 7 and kept in a safe place free from UV radiations. A schematic representation of the synthesis of cobalt complex ($Na_3[Co(CO_3)_3].3H_2O$) to its convertion to diaquo complex $[Co(tn)_2(OH_2)_2]^{3+}$ is shown below:

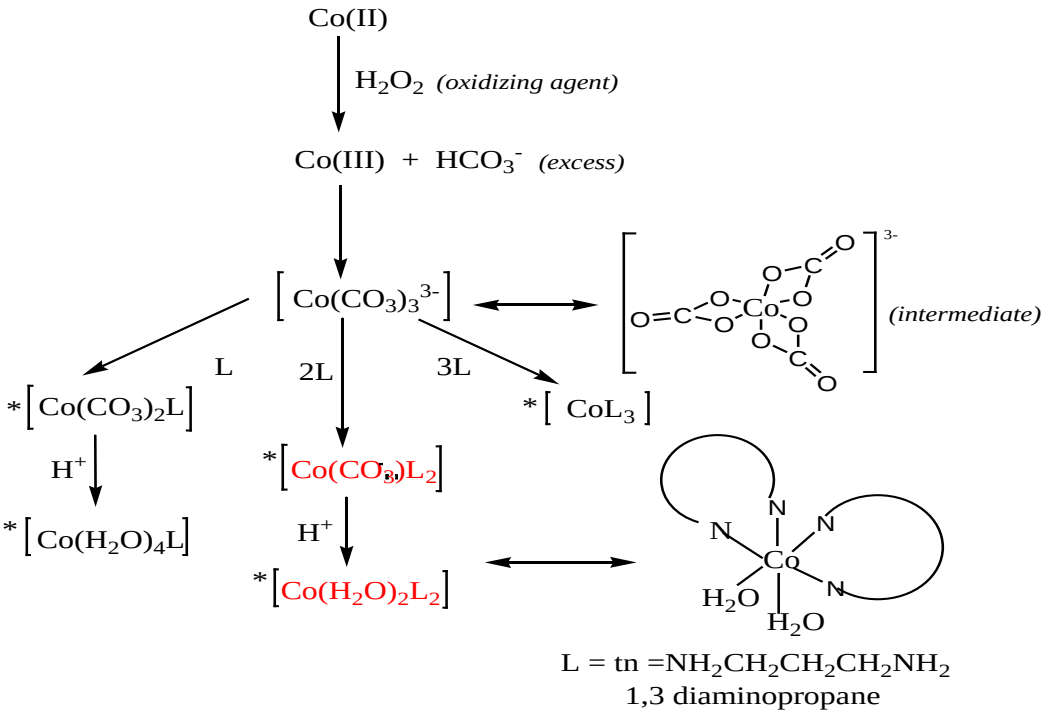

.

Scheme 2.0 Schematic representation of the Co(III) complex synthetic pathway.

(*The charges on the complexes are omitted for clarity. This is because the charges on the ligands are unspecified)

2.3 PROTOCOL OF THE STUDY

Our investigation was undertaken using two method of analysis namely; the nitrophenolate method and the phosphate determination method. P-nitrophenylphosphate on dephosphorylation produces p-nitrophenolate ion and a phosphate moiety. The nitrophenolate method explains procedures used in obtaining and measuring the p-nitrophenolate ion produced in the reaction. The phosphate determination methods takes into account the measurement of the amount of inorganic phosphate produced in the solution as a result of dephosphorylation. For clarity sake we will discuss each method distinctively and show results in subsequent chapters.

2.3.1 THE NITROPHENOLATE PROTOCOL

It involves mixing 2mL of an aqueous solution of 5 x 10^{-3}M p-nitrophenylphosphate (NPP) in a thermostated reaction vessel, housed in the fluorescence analysis cabinet, with 6mL of water. The pH of the solution was adjusted to 7. A 2mL volume of temperature equilibrated sodium nitroprusside solution (our nitric oxide source) (5 x 10^{-3}M, pH of 7) was then added making the total volume 10mL.The light source was then turned on and aliquots (1mL) were drawn from the reaction vessel at 0.5, 1, 1.5, 2, 2.5, 3, 5, 10, 15….120 minutes. The aliquots were mixed with 1mL of phosphate buffer (pH 7.4) and 3mL of H_2O, absorbance values of the reaction solution on each case were measured at 400nm.

Nitrophenolate ion determination requires a buffered system, in the sense that in an unbuffered solution, the acid-base reaction of the 4-nitrophenol changes in concentration resulting in a shift in the equilibrium position and a consequent deviation from Beer's law as depicted below.

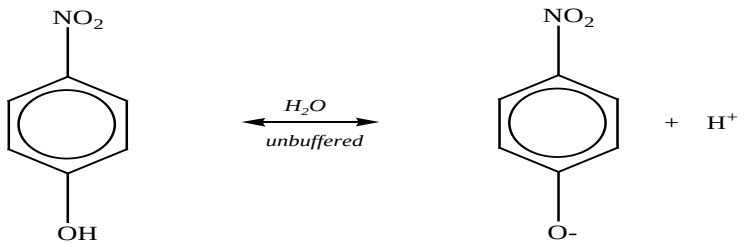

In a buffered system, the pH of the solution remains fixed and the ratio of the concentration of the p-nitrophenolate ion to the p-nitrophenol would be constant thereby obeying Beer's law. Hence, the buffer solution was introduced to create stability in the monitoring of the nitrophenolate ion production in the system. The buffer was prepared by mixing 8.62g of sodium phosphate dibasic and 5.42g of sodium phosphate monobasic salts and making up the volume to 1000mL with carbondioxide free distilled water.

In the reaction solutions, nitric oxide was obtained by the photolysis of sodium nitroprusside $Na_2[Fe(CN)_5NO]\cdot 2H_2O$. This reaction was measured by monitoring the amount of aquacyanoferrate ion $[Fe(CN)_5(H_2O)]^{2-}$ produced in solution. The nitrophenolate ion to be measured as a result of dephosphorylation and the aquacyanoferrate ion obtained as a result of photolysis of sodium nitroprusside are both measured at 400nm with the UV-visible spectrophotometer. Since our ions of interest absorbs at same wavelength, an interference study was done using sodium nitroprusside which is measured at 400nm, incorporation our method of analysis. A 5×10^{-3}M solution of SNP was prepared and photolysed according to the experimental protocol described above. The absorbance values of the aquacyanoferrate ion measured for the reaction times (5-120 min) were documented and subsequently subtracted from the values obtained in the experiment with both 4-nitrophenylphosphate and sodium nitroprusside. This blanked the effects of the aquacyanoferrate ion in the reaction. The net absorbance used in calculating the percentage hydrolysis being solely obtained as a result of dephosphorylation (nitrophenolate ion production).

A 5×10^{-3}M solution of p-nitrophenol was subjected to same explained protocol and the results documented. The percentage hydrolysis was calculated as a ratio of the net absorbance values of the reaction aliquots over the absorbance value of 5×10^{-3}M p-nitrophenol multiplied by 100. Triplicate analysis was done for each system to distribute errors. The standard deviation for the triplicate analysis ranged from 0.1 to 0.2 in each case. The average value was used for analysis of data and results, and all absorbance were taken against water used as blank.

Similarly 1:1, 2:1 and 3:1 solutions of $[Co(tn)_2(OH_2)_2]^{3+}$: NPP ratios were prepared in a volume of 10mL. When the system has reached saturation in about 5 minutes, 2mL of temperature equilibrated sodium nitroprusside (5×10^{-3}M, pH 7.0) was added and photolysed. Production of nitrophenolate ion with time was then monitored and the result documented. Again, A 5×10^{-3}M solution of sodium nitroprusside $Na_2[Fe(CN)_5NO]\cdot 2H_2O$ was subjected to same explained protocol and the absorbance values of the aquacyanoferrate ion $[Fe(CN)_5(H_2O)]^{2-}$ deducted from the values of the reaction times (5-120 min.). The net value used to calculate the percentage hydrolysis assuming 100% nitrophenolate ion production for complete dephosphorylation. Reactions containing higher ratio of nitric oxide was achieved by using 4mL and 6mL of SNP. All reactions were designed so that the final concentration prior absorbance reading was 1×10^{-3}M solution, they were monitored and result documented.

At higher values of sodium nitroprusside (our nitric oxide donor), large interference values obtained for aquacyanoferrate ion $[Fe(CN)_5(H_2O)]^{2-}$ becomes prominent. The nitrophenolate ions produced in reaction solutions were been overshadowed by high value of the aquacyanoferrate ions in the solutions. This necessitates an alternative method of monitoring the reactions that involves increased amount of sodium nitroprusside. We decided to monitor the amount inorganic phosphate produced in solution on dephosphorylation. This method is unique and advantageous in that it takes care of the interference problems associated with nitrophenolate ion and aquacyanoferrate ion, since inorganic phosphates in solution can be monitored at a different wavelength.

2.3.2 PHOSPHATE DETERMINATION METHOD – AN OVERVIEW

Inorganic phosphates react with molybdate in strong acid solution to produce heteropoly molybdate. A good example is the yellow ammonium phosphomolybdate, $(NH_4)_3PMo_{12}O_{40}$. The phosphorus atom in the anion is termed the hetero-atom [90]. The heteropoly-molybdenum compounds have structures based on the keggin structure. A phosphate sample mixed with acid solution of Mo^{VI} (ammonium molybdate) produces phosphomolybdate anion, $PMo_{12}O_{40}^{3-}$. This anion have an α- keggin structure [91]. This

anion reduced by ascorbic acid or $SnCl_2$ to a molybdenum blue compound with uncertain concentration ratio of Mo (IV) and Mo (VI) produces a β- keggin ion $PMo_{12}O_{40}^{7-}$ with maximum absorption at 885nm [92]. The amount of the blue colored ion produced is proportional to the amount of phosphate present. The blue color arises because the near colorless phosphomolybdate anion, $PMo_{12}O_{40}^{3-}$ can accept more electrons (to be reduced) to form an intensely colored mixed valence complex. This can occur in one electron or two electron steps. The reduction process is reversible and the structure of the anion is essentially unchanged [93].

$$PMo_{12}^{VI}O_{40}^{3-} + 4e \rightleftharpoons PMo_4^{V}Mo_8^{VI}O_{40}^{7-} \quad \text{.....21}$$

The anion $PMo_4^{V}Mo_8^{VI}O_{40}^{7-}$ has been determined in solid state and is a β- isomer i.e. with one of the four groups of edge shared octahedra on the α- keggin ion rotated through 60 degrees [92].

2.3.2.1 THE KEGGIN STRUCTURE

This is the best known structural form for heteropoly acids. It is the structural form of α-keggin with general formula $[XM_{12}O_{40}]^{n-}$, where X is the heteroatom usually P^{5+}, Si^{4+} or B^{3+}, M is the addenda atom (in this case molybdenum) and O represents oxygen. This structure self assembles in acidic aqueous solution and is the most stable structure of the polyoxometalate catalysts [94]. Isomerism occurs in the α-keggin structure to give rise to different forms of structures designated by the prefixes β-, γ-, δ-, ε-. They are all derived from α- structures and their differences arises from different rotational orientations of the Mo_3O_{13} units which lowers the symmetry of the overall structure [95].

In our solution, the heteroatom is the free phosphate – orthophosphate (phosphorus surrounded by oxygen to form a tetrahedron). It is located centrally and caged by 12 octahedral MoO_6 units linked to one another by the neighboring oxygen atoms. There are a total of 24 bridging oxygen atoms that linked the 12 molybdenum (addenda) atoms. The metal centers in the 12 octahedra are arranged on a sphere almost equidistant from each other, in four Mo_3O_{13} units giving the complete structure an overall tetrahedral symmetry

as depicted below.

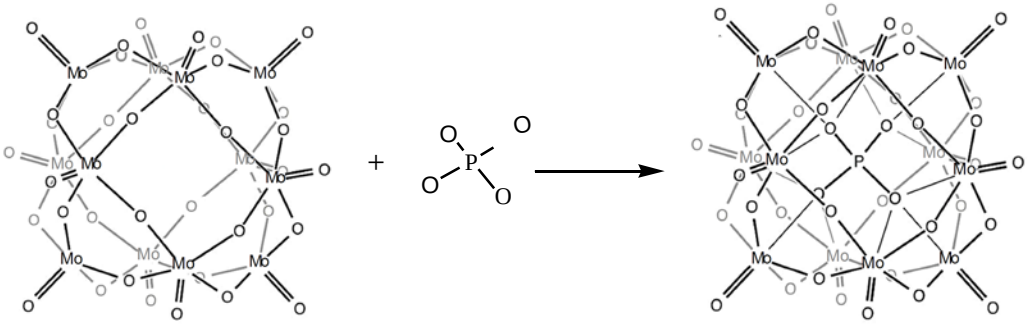

The above shows a phosphate reaction with ammonium molybdate to give α- keggin phosphate-molybdate ion. The color formation is due to the reduction of α- keggin phosphate-molybdate ion ($PMo_{12}O_{40}^{3-}$) to blue colored β- keggin ion ($PMo_{12}O_{40}^{7-}$) by ascorbic acid. A brief description of the analytical method utilized in the determination of inorganic phosphate produced in solution is discussed below.

2.3.2.2 ANALYTICAL METHOD FOR PHOSPHATE DETERMINATION

Colorimetric method that utilizes an insitu formation of reduced heteropoly acid complex was developed from literature [96]. The blue heteropoly acid has a maximum absorbance at 885nm. The intensity of the blue solution is related to the concentration of the phosphate in the sample. Based on these, the following reagents were prepared:

(a) Ammonium Paramolybdate solution [$(NH_4)_6Mo_7O_{24}.4H_2O$], 0.025M.

15 grams of ammonium paramolybdate was dissolved in 500mL of distilled water. The solution stored in a dark plastic bottle is stable and can be reused.

(b) Sulphuric acid solution (H_2SO_4), 2.5M.

140mL of concentrated sulphuric acid was added to 900mL of distilled water. The solution was allowed to cool at room temperature and stored in a glass bottle.

(c) Ascorbic acid solution ($C_6H_8O_6$), 0.3M.

27 grams of ascorbic acid was dissolved in 500mL of distilled water. This was stored in a plastic bottle and kept in a freezer. It was thawed before use.

(d) Potassium antimonyl-tartrate solution ($C_8H_4K_2O_{12}SB_2.3H_2O$), 4 x 10^{-3}M.
0.68 grams of the solid was dissolved in 250mL of distilled water.

(e) Sodium dihydrogenphosphate solution ($NaH_2PO_4.2H_2O$), 6.0 x 10^{-3}M.
0.935 grams of $NaH_2PO_4.2H_2O$ was dissolved in 1000mL of distilled water. It was stored in a dark bottle with 1mL of chloroform added as a preservative. The phosphorus concentration was determined using $NaH_2PO_4.2H_2O$ as a primary standard.

(f) Mixed reagent (to be used for analysis).
The following composition by volume of the above reagents (a-d) were mixed to give the reagent solution that was utilized for the analysis; 100mL of ammonium molybdate solution (reagent a), 250mL of sulphuric acid (reagent b), 100mL of ascorbic acid (reagent c) and 50mL of potassium antimonyl-tartrate solution (reagent d), the mixed reagent was used within six hours of constitution.

The analysis involves the mixing of 10 part of the analyte to 1 part of the mixed reagent. The mixture was allowed to stand for at least five minutes before its absorbance was read at 885nm against a blank which contained 10 part of distilled water to 1 part of the mixed reagent. Absorbance measurements were taken within 2 hours after the addition of the mixed reagent. A detail of the protocol employed is depicted below.

2.3.2.3 PHOSPHATE DETERMINATION PROTOCOL

The protocol of the study consist of mixing 2mL of an aqueous solution of a 5 x 10^{-3}M of the model organophosphate (NPP/PPi) in a thermostated vessel, housed in a fluorescence analysis cabinet, with 6mL of water. The pH of the solution was adjusted to 7. A 2mL volume of temperature equilibrated sodium nitroprusside (5 x 10^{-3}M); pH 7 was then added, making the total volume to 10mL.
The light source was then turned on and aliquots (1mL) were drawn from the reaction vessel at several intervals (1, 2, 3, 5, 10, 15, 20……..120 minutes). The aliquots were mixed with 9mL of distilled water and 1mL of the mixed reagent added to it and mixed well. The absorbance measurement was done at 885nm. The percentage hydrolysis was

calculated assuming 100% inorganic phosphate production for complete hydrolysis. Triplicate analysis was done for each system. The standard deviation for the triplicate analysis ranged from 0.1 to 0.2 in each case. The average value was used for analysis of the data.

Similarly 1:1, 2:1 and 3:1 solutions of $[Co(tn)_2(OH_2)_2]^{3+}$: NPP/PPi ratio was prepared in a total volume of 10mL. When the system reached saturation in about 5 minutes, 2mL of temperature equilibrated sodium nitroprusside solution (5 x 10^{-3}M, pH 7) was added and photolysed. For a higher ratio of sodium nitroprusside, 4mL and 6mL of the solution were utilised. Production of inorganic phosphate with time was then monitored and percentage hydrolysis calculated.

Phosphoric acid speciation in aqueous solution at different pH values is depicted in figure 2.1 [90].

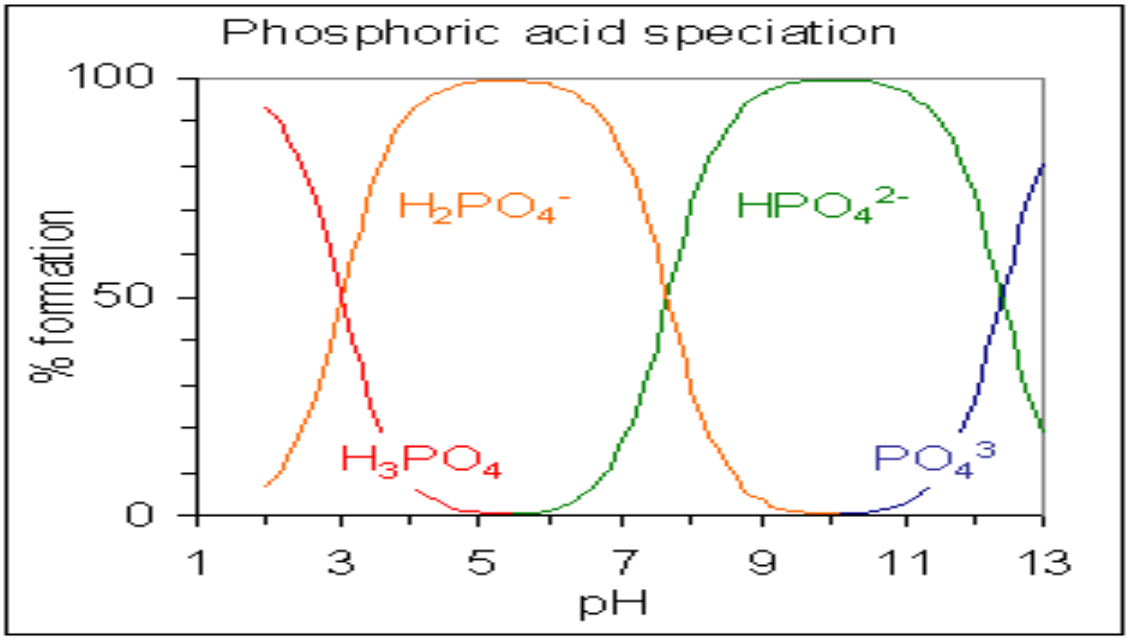

Figure 2.1 Percentage phosphate species formation as a function of pH.

The reaction between NPP/PPi and nitric oxide was performed and results documented for both the nitrophenolate protocol and the phosphate determination method. Also the same protocols were utilized for the reaction of cobalt(III) complex $[Co(tn)_2(OH_2)_2]^{3+}$,

NPP/PPi and nitric oxide. Triplicate analysis for each system was obtained and the average value was used for the results shown in the subsequent chapter.

CHAPTER THREE

3.0 RESULTS AND DISCUSSION

The results obtained in these experiments will be shown with respect to the different experimental protocols involved. The discussion follows subsequently.

3.1 PHOTOLYSIS OF AQUEOUS SOLUTION OF SODIUM NITROPRUSSIDE

A 5 x 10^{-3}M aqueous solution of $Na_2[Fe(CN)_5NO]$, initial pH of 7 was subjected to irradiation at 254nm, 365nm and white light in a thermostated reaction vessel with continuous stirring, housed in a photolysing cabinet. One millilitre of aliquot was withdrawn with time in accordance with the protocol of the study and absorbance measured at 400nm. The pH profile was also monitored for the entire reaction period. The result is depicted in figure 3.0.

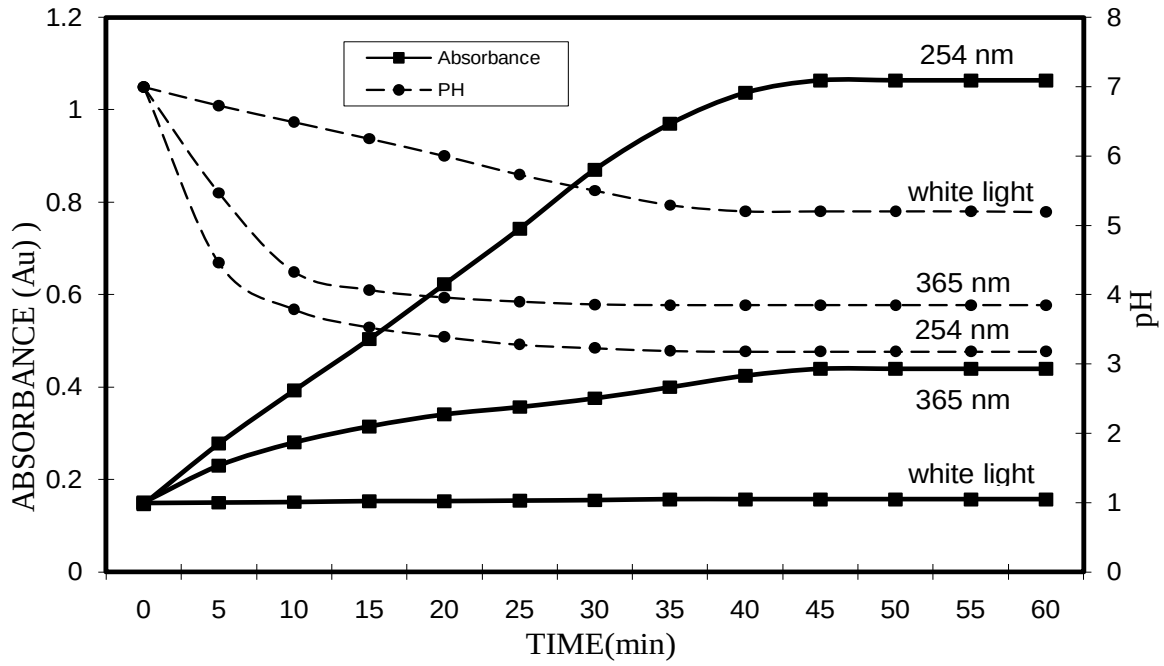

Figure 3.0: Absorbance measurement and pH profile for the photolysis of 5 x 10^{-3}M aqueous solution of [$Na_2[Fe(CN)_5NO]$ at 254nm, 365nm and white light with time at 400nm (25^{o}C and initial pH of 7).

The photosensitivity of aqueous solution of $Na_2[Fe(CN_5)NO]$ has long been recognized [86]. Figure 3.0 shows absorbance measurement and pH profile for the photolysis of 5 x 10^{-3}M aqueous solution of $Na_2[Fe(CN)_5NO]$ using 254nm 365nm UV irradiations and white light. The results obtained were measured at 400nm with a UV-vis spectrophotometer. The production of nitric oxide in the reaction was indirectly monitored by measuring the amount of aquacyanoferrate ion $[Fe(CN)_5(H_2O)]^{2-}$ produced in the solution which has maximum absorption at 400nm as shown in equation 18. Furthermore, the decrease in the pH of the photolysed solutions for the different wavelengths of irradiation proves that the primary process of photolysis of SNP involves the production of nitric oxide and aquacyanoferrate ion. The 254nm irradiated solutions showed marked difference and increase in nitric oxide production compared to the 365nm irradiated solutions. The pH of the reaction solutions also showed significant decrease. The white light irradiated reaction solutions did not show significant production of nitric oxide.

The results obtained for this experiment were the values of the aquacyanoferrate ion which must be deducted from the values obtained due to dephosphorylation at different reaction times. By subtracting these values from our reaction results, the interference from the aquacyanoferrate ion is taken care of and the net absorbance values obtained will be solely due to dephosphorylation. Since there is marked difference in nitric oxide production in solution using the 254nm UV irradiation, subsequent experiment were conducted using this wavelength of irradiation.

3.2 SODIUM NITROPRUSSIDE ASSISTED DEPHOSPHORYLATION OF 4-NITROPHENYLPHOSPHATE: THE NITROPHENOLATE PROTOCOL

The dephosphorylation reaction of 1 x 10^{-3}M aqueous solution of 4-nitrophenylphosphate with an equimolar amount of aqueous sodium nitroprusside was studied under 254 and 365nm photolysis. A 2:1 molar ratio of SNP: 4-NPP reaction solution was also subjected to similar study. Nitrophenolate ions produced were monitored. The obtained results are shown in figure 3.1 overleaf.

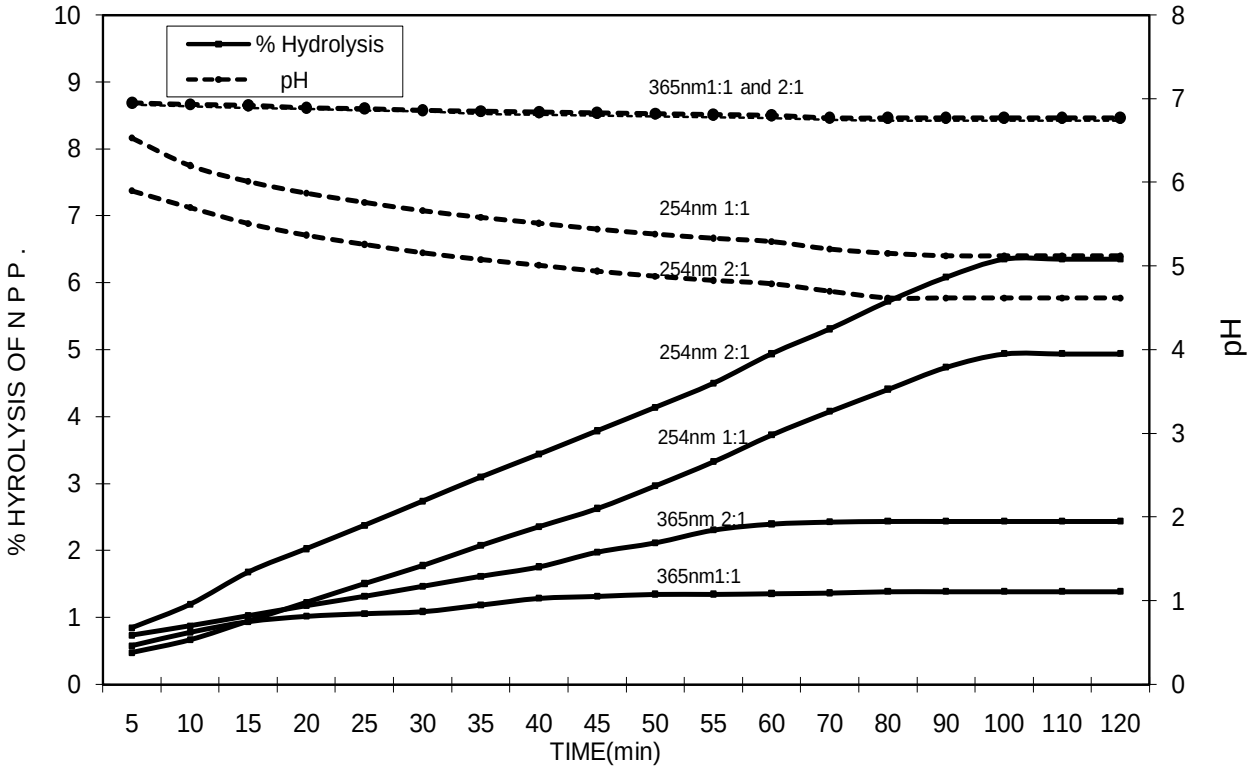

Figure 3.1 Percentage hydrolysis and pH profile for the reaction of 1 x 10^{-3}M aqueous solution of 4-nitrophenylphosphate with 1 x 10^{-3}M aqueous solution of $Na_2[Fe(CN)_5NO]$ at 254nm and 365nm UV photolysis for 1:1 and 2:1, SNP:4-NPP ratio at 25^{o}C and initial pH of 7 using the nitrophenolate method.

The above result shows dephosphorylation reactions observed for 1:1 and 2:1 SNP: NPP ratio under both 254nm and 365nm irradiations. As can be seen from the figure, there is an increase in nitrophenolate ion production as we go from the 1:1 to the 2:1 SNP to NPP ratios for both the 254nm and 365nm irradiated solutions. The results obtained for white light mediated reactions were insignificant (less than 1%) so they were not depicted in the figure. The pH profile for all the results shown in the figure consistently showed a decrease as the reaction was conducted, this signifies dephosphorylation reactions. This result can be explained by similar study conducted by Kuhn [97] in his reaction of nitric oxide and triethylphosphite to yield nitrous oxide and triethylphosphate as it showed similar trends. A mechanism was proposed by him for the reaction he conducted which involves the intermediate $(EtO)_3PNO$. Based on the similar documented literature, the

following reaction mechanism was proposed for the reaction of nitric oxide with nitrophenylphosphate.

$[Fe(CN)_5(NO)]^{2-} + H_2O \longrightarrow [Fe(CN)_5(H_2O)]^{2-} + NO$ 22

$NO + NPP \longrightarrow (NPP)ON$ 23

$(NPP)ON + NO \longrightarrow NP + Pi + N_2O$ 24

The structure of the intermediate can be pictured as (NPP)ON in which the oxygen of the second nitric oxide molecule would produce nitrous oxide. Alternatively, the intermediate structure would be (NPP)N=O and the oxygen of the second nitric oxide becomes bound to the phosphorus center thereby resulting in the release of nitrous oxide.
This reaction can be represented diagrammatically below.

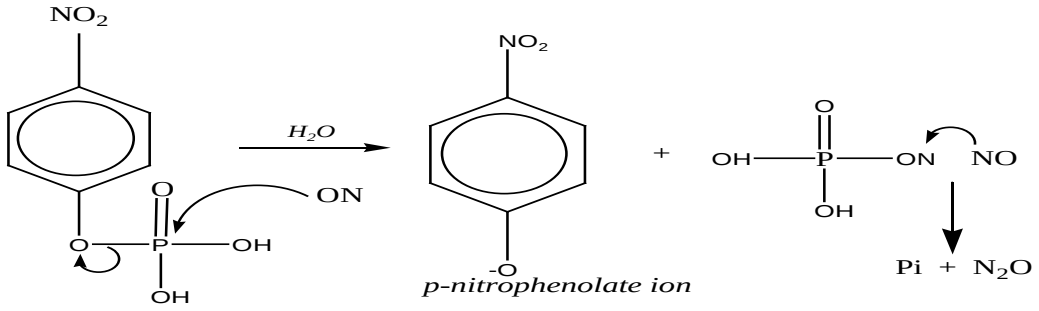

The degree of dephosphorylation seems to be proportionally related to the amount of nitric oxide available in the reaction which is governed by the mode of irradiation.
This is quite noted in the reactions involving different source of irradiation. The 254nm irradiated solutions showed appreciable increase in dephosphorylation compared to the 365nm irradiated solutions.
A further attempt to increase the amount of nitric oxide (3:1 SNP: NPP ratios) by stoichiometrically increasing the amount of SNP did not yield positive results. The increased amount of SNP in the reaction solution leads to the formation of large amounts of aquacyanoferrate ion $[Fe(CN)_5(H_2O)]^{2-}$ which contributes hugely to the absorbance at 400nm. The large values of the blank absorption mask the additional absorption of the nitrophenolate to be detected in the reaction as a result of dephosphorylation, so the

results of the reactions could not be effectively calculated at high concentrations of SNP.

3.3 SODIUM NITROPRUSSIDE PROMOTED DEPHOSPHORYLATION OF PREFORMED COBALT (III) NITROPHENYLPHOSPHATE COMPLEXES AT 254NM UV RADIATION: THE NITROPHENOLATE PROTOCOL

The dephosphorylation reactions of NPP promoted by $[Co(tn)_2(aq)]^{3+}$ has been the subject of study in our laboratory for quite some time [7, 8]. The reactions show rate saturation within 1 minute of addition of the cobalt complex into the aqueous solution of NPP. A schematic representation of the Co(III) complex synthetic pathway is shown in scheme 2.0. It shows the CoL_3, $Co(H_2O)_4L$ and $Co(H_2O)_2L_2$ complex formations, where the ligand (L) is tn (1,3 diaminopropane). In the CoL_3 complex formation, the six coordination sites are presumed to be fully occupied by the bidentate ligand. Hence, hydrolytic action is not expected in this system. In the $Co(H_2O)_2L_2$ complexes, it is assumed that four of the six coordination sites of cobalt have been occupied by two of the bidentate ligand, thus allowing the remaining two sites to be occupied by water. Our cobalt complex was duly prepared to fit this ratio. In the solution of this type the diaqua, hydroxoaquo and the dihydroxo species exist in solution depending on the pH of the reaction solution. The predominance of the hydroxo-aqua species in the pH ranges of 4-8 and the existence of isosbestic points in the UV-visible spectra studies of $[Co(tn)_2(aq)]^{3+}$ complexes has been documented [8]. The existence of an isosbestic point is often considered proof of the presence of two absorbing species in the analysed solution [98-99]. Hence, the presence of both hydroxoaqua and diaqua species is predicted to prevail between the pH ranges of 4-6 and the hydroxoaqua and dihydroxo species between the pH ranges of 6-8. It is presumed that at pH around 7.0, the hydroxoaqua species is predominant. Literature values of pk_1, 4.98 and pk_2, 7.22 for $[Co(tn)_2(H_2O)_2]^{3+}$ support the above assumption [100]. Hence, at pH of around 7.0 the $[Co(tn)_2(OH)(H_2O)]^{2+}$ and NPP react to form a cis hydroxo monodentate-NPP specie. The literature shows that $[Co(tn)_2(OH)(H_2O)]^{2+}$ exists almost exclusively in cis form in aqueous solutions [101].

2mL of 5 x 10^{-3}M aqueous solution of 4-nitrophenylphosphate was mixed with the same amount and molar concentration of aqueous $[Co(tn)_2(aq)]^{3+}$ in a thermostated reaction vessel and the volume made up to 10mL and pH adjusted to 7. The compound produces a solution which is 1 x 10^{-3}M in $Cotn_2$NPP complex. Similarly, addition of 2mL of 5 x 10^{-3}M aqueous solution of 4-nitrophenylphosphate with 4mL of 5 x 10^{-3}M aqueous solution of $[Co(tn)_2(aq)]^{3+}$ produces a solution which is 1 x 10^{-3}M in $(Cotn_2)_2$NPP complex. After 5 minutes of reaction, 2mL of 5 x 10^{-3}M aqueous solution of $Na_2[Fe(CN)_5NO]$, initial pH of 7 was added and irradiation at 254nm resumed. Production of nitrophenolate ion was monitored at 400nm during the formation of the cobalt complexes (i.e. 0-5min) and after the resumption of the photolysis of sodium nitroprusside (5-120min). The result is shown in figure 3.2 below.

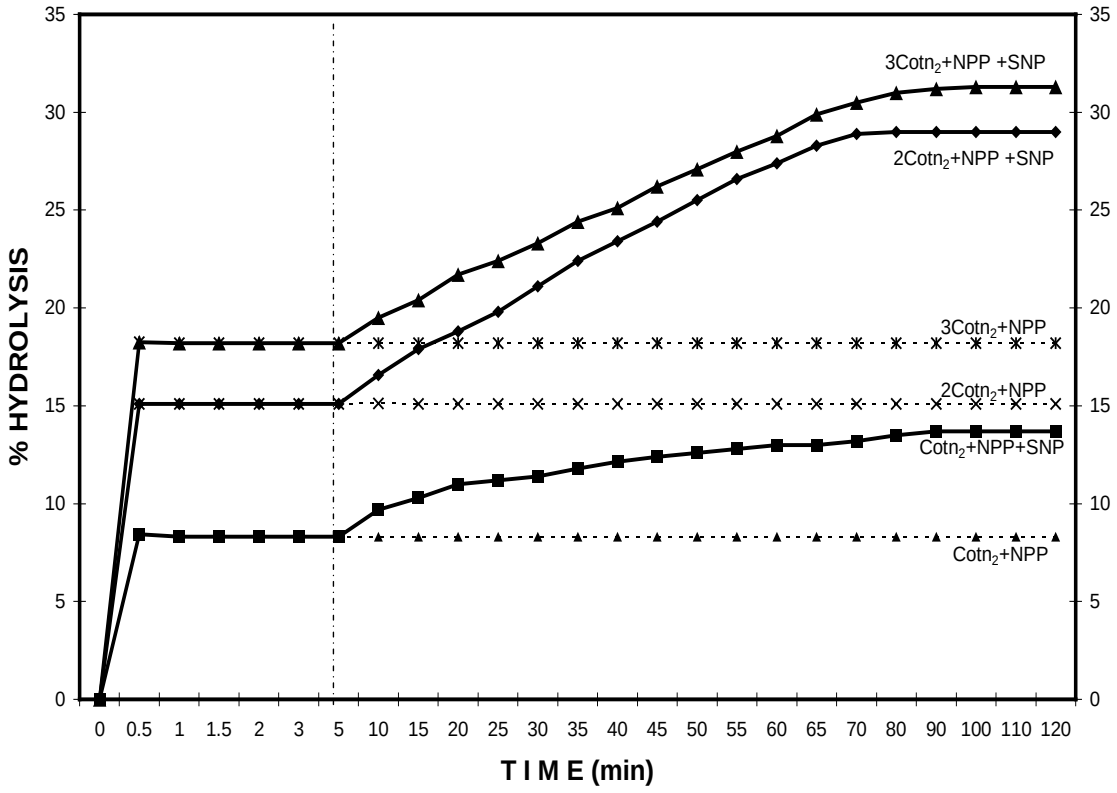

Figure 3.2 Percentage hydrolysis for the reaction of preformed 1 x 10^{-3}M $Cotn_2$NPP complexes (1:1, 2:1 and 3:1; $Cotn_2$:4NPP ratio) with 1 x 10^{-3}M aqueous solution of $Na_2[Fe(CN)_5NO]$ at 254nm UV photolysis (25^{o}C and initial pH of 7) using the nitrophenolate method.

The reaction of preformed $Cotn_2NPP$ and NO as depicted in figure 3.2 can be explained in two phase of reactions. In both phases the amount of nitrophenolate ion produced in solution was monitored. The first phase shows a pH rise from reaction time of 0 to 1 minute possibly due to $[Co(tn)_2(aq)]^{3+}$ reaction with NPP to form $Cotn_2NPP$ complex and inevitably the intramolecular attack by the coordinated hydroxide of the cobalt complex on the phosphorus, thereby promoting dephosphorylation of the NPP as shown in the resulting figure 3.2. The reaction was allowed to saturate for 5 minutes possibly enhancing more $Cotn_2NPP$ complex formations in the system. The second phase of the reaction was the addition of SNP after 5 minutes of $Cotn_2NPP$ formation. An increase in the dephosphorylation was noted which levels out after about 60-80 minutes of reaction time for all SNP to NPP ratios. It may be worthy to note that nitric oxide can trigger possible attack on the phosphorus centre thereby taking credence for the rate enhancement observed in this phase of the reaction. A plausible mechanism for this reaction is shown below.

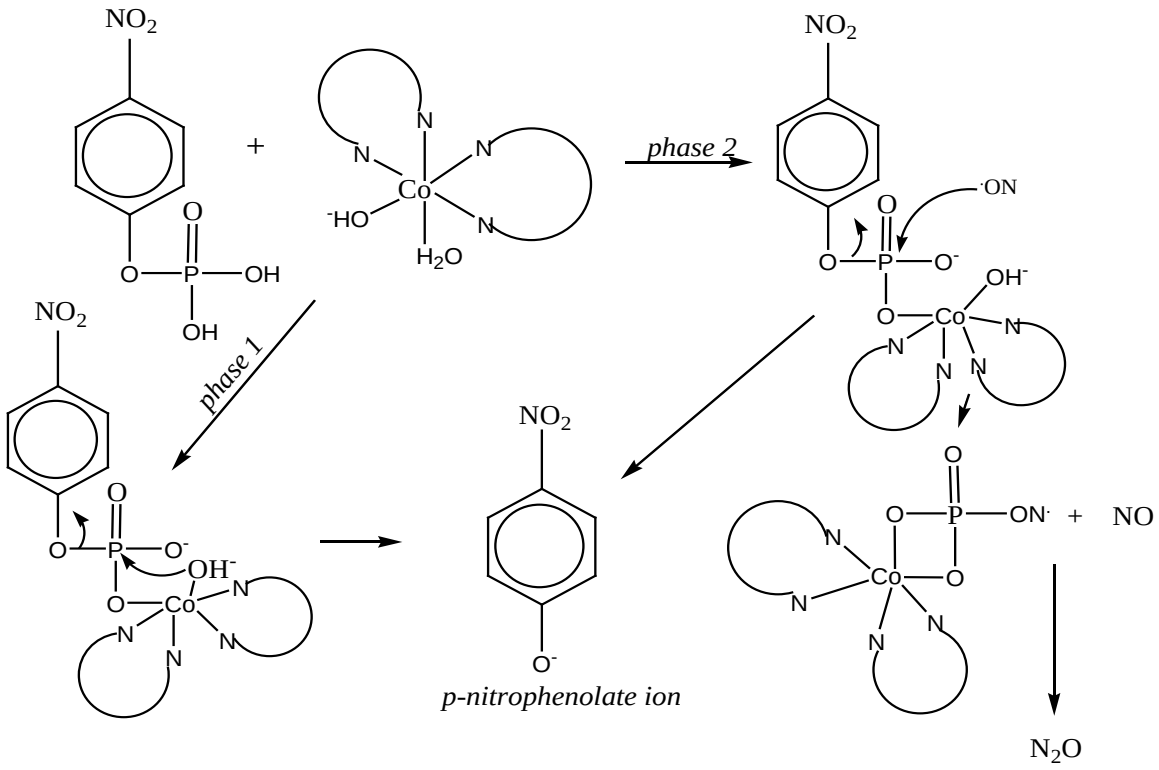

Scheme 3.0 Plausible mechanism of nitric oxide triggered dephosphorylation of $Cotn_2NPP$ complexes.

In the reactions explained, the SNP and NPP ratios were kept constant at one molar as the $[Co(tn)_2(aq)]^{3+}$ was increased from one molar to three molar ratios. There is roughly a two fold increase in nitrophenolate ion production noted for the $2Cotn_2$ + NPP + SNP reactions compared to what we obtained for the $Cotn_2$ + NPP +SNP reactions. In the first phase of the reaction (0 to 5 minutes), that is the addition of the cobalt complex to the NPP solution. An enhancement in dephosphorylation was noted in reaction solutions that contained 2:1 metal to NPP ratio. This can be explained by the fact that the second metal ion coordinates to one of the available oxygen on the NPP, thereby creating a possibility of intramolecular attack on the phosphorus centre by coordinated water or hydroxide of the metal ion. The second phase of the reaction (which is the addition of SNP, our nitric oxide donor), recorded increased in dephosphorylation in the system that contained 2:1 metal to NPP ratio. A possible explanation is that the increase in the positive character of the phosphorus centre as a result of coordination of its oxygen to two cobalt complexes enhances an attack on the phosphorus centre by the nitric oxide moiety, thereby leading to further dephosphorylation as seen in figure 3.2.

The observed reaction of the 3:1 molar ratio solutions of $[Co(tn)_2(aq)]^{3+}$ and NPP were not markedly different from those of 2:1 since there are no available oxygen for $[Co(tn)_2(aq)]^{3+}$ coordination in the NPP compound . It is expected that the 2:1 moieties will predominate in the solution in the 3:1 reaction systems. Hence its mode of reactivity with nitric oxide will not be much different compared to the 2:1 system. The pH profile showed an increase to 7.6 during the first phase (0-5 minutes) of the reaction and consistent decrease during the second phase (5-120 minutes) to 6.8. All solutions had pH adjusted to 7 at starting of reactions. An increase in pH is attributed to complex formation while a decrease in pH is presumably due to dephosphorylation reactions. A decrease in pH in all cases were noted during the progress of the reaction, but since we were able to monitor the reaction after some minutes, the pH lines on the figures do not start at the value of 7 and the pH varies for different systems studied. An average for the systems studied were taken and plotted accordingly.

Subsequent experiments performed were conducted by monitoring the amount of phosphate produced in reaction solutions. We used the colorimetric protocol as described in the analytical method for phosphate determination (2.3.2.2). Again, the shift from monitoring the nitrophenolate ion to monitoring the amount of phosphate produced in reaction solutions was necessary to circumvent the problem that arises from huge aquacyanoferrate ion $[Fe(CN)_5(H_2O)]^{2-}$ absorption which masked the effects of higher mole ratios of SNP since both ions absorbs at wavelength of interest.

3.4 CALIBRATION CURVE STUDIES FOR NaH_2PO_4 (STANDARD)

The phosphate determination method requires a reference phosphate standard from which the concentration of our phosphate in solution can be calculated. In this study, we used NaH_2PO_4 as our phosphate standard. This standard solution was prepared within our concentration of interest and a plot of concentration vs. absorbance was obtained.

Solutions of NaH_2PO_4 were prepared in different concentration ranges using known procedures. Absorbance values of the standard were recorded from concentration ranges of 1µM -30µM using the UV-vis spectrometer at 885nm. A plot of concentration Vs absorbance gives the regression equation $Y = mx + b$ from which the concentration of phosphate in our samples can be calculated by plugging the absorbance values of x in the regression equation. Figure 3.3 below show the calibration curve study using NaH_2PO_4 standard.

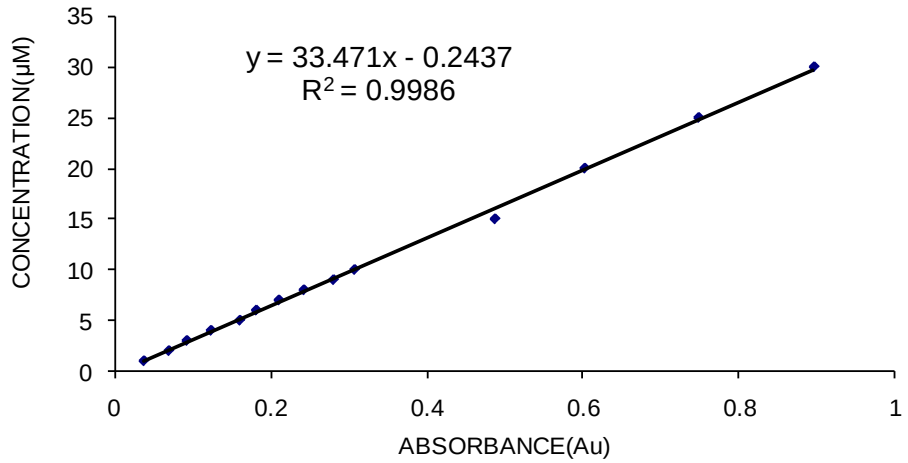

Figure 3.3 Calibration curve for NaH_2PO_4 standard within concentration range of 1µM-30µM.

It should be noted that the plots were deliberately inverted for convenience. Using the regression equation y = mx + b, m conforms to the value 1/ε following Beer's law in the calculation of the concentration of the samples due to absorbance.

For example, using the value of 0.031 for a net absorbance reading of a particular time (t_1), the percentage hydrolysis is calculated as follows;

Calibration curve shows that 1/ε is 33.471. Concentration in molar = A/ε x L (Beer's law)

Concentration (M) = $0.031 \times 33.471 \times 10^{-6} = 1.038 \times 10^{-6}$M

Multiplication by 10^{-6} gives the concentration in molar since the standard was prepared in µM and the path length of the cuvette being 1.
The percentage hydrolysis was calculated as;

$$\% \text{ Hydrolysis} = \frac{\text{Concentration (M)}}{1.000 \times 10^{-4}} \times \frac{100}{1}$$

$$\Rightarrow \frac{1.038 \times 10^{-6}}{1.000 \times 10^{-4}} \times \frac{100}{1} = 1.038\%$$

Where, 1.000×10^{-4}M (0.00009091) was the final concentration of the sample prior

absorbance measurement. The percentage hydrolysis was calculated for all the experiments using the above shown calculation for each net absorbance value obtained for the different reaction time (0- 120 minutes). The results were plotted against different reaction times and shown accordingly.

3.5 SODIUM NITROPRUSSIDE ASSISTED DEPHOSPHORYLATION OF 4-NITROPHENYLPHOSPHATE: PHOSPHATE DETERMINATION METHOD

The dephosphorylation reaction of 1 x 10^{-3}M aqueous solution of 4-nitrophenylphosphate with an equimolar amount of aqueous sodium nitroprusside was studied under 254nm photolysis. A 2:1 and 3:1 molar ratio of SNP: NPP reaction solutions were also subjected to similar study. In these reactions the inorganic free phosphate produced as a result of dephosphorylation was monitored. The results and pH profile are shown in figures 3.4 below.

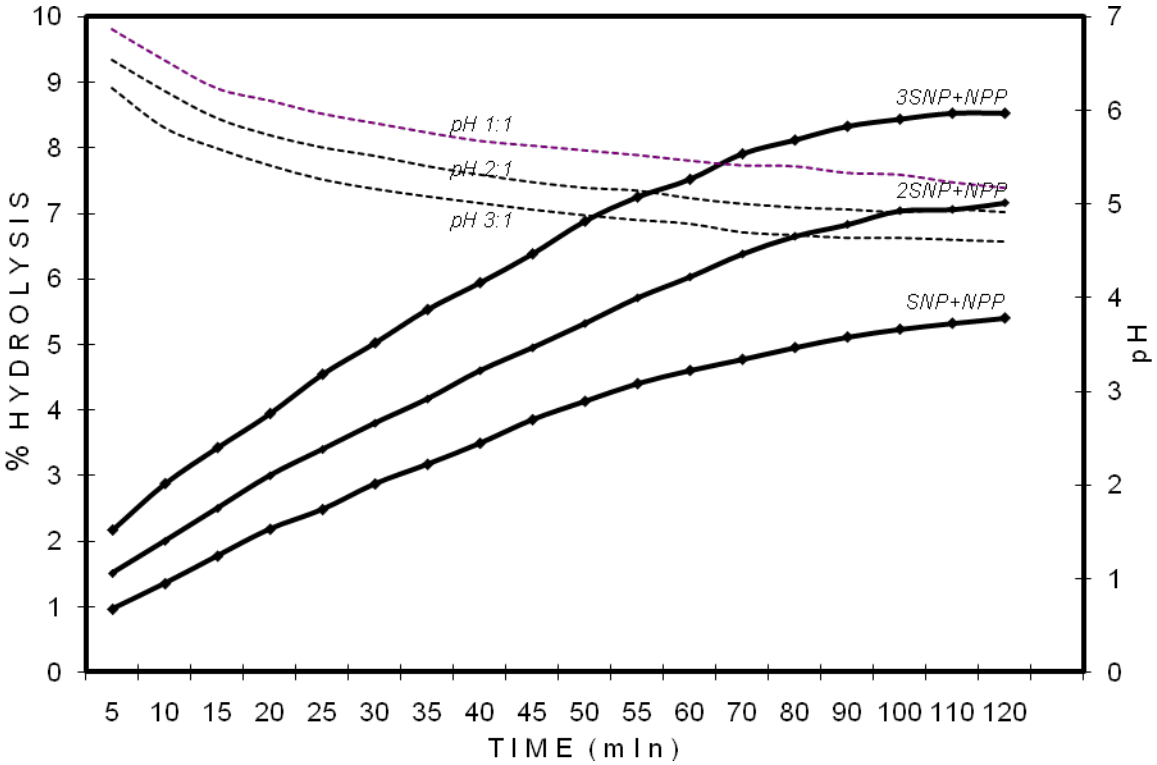

Figure 3.4 Percentage hydrolysis and pH profile for the reaction of 1 x 10^{-3}M aqueous solution of 4-nitrophenylphosphate with 1 x 10^{-3}M aqueous solution of $Na_2[Fe(CN)_5NO]$ at 254nm for 1:1, 2:1 and 3:1; SNP:NPP ratio at 25^{o}C and initial pH of 7 using phosphate determination method.

The result shown in figure 3.4 demonstrates that there is an increase in hydrolysis for systems that contains more nitric oxide. The results were obtained by using only the 254nm irradiation. It clearly showed that chances of attack on the phosphorus centre increase proportionally with nitric oxide concentration. This would account for the added dephosphorylation products in the reaction. The results obtained for figures 3.1 and 3.4 reasonably correlate. There is an increase in dephosphorylation as SNP to NPP ratio increases stoichiometrically. The pH of both reactions showed similar trends also.

The increased results masked in figure 3.1 can be clearly seen in figure 3.4 as the phosphate produced can be measured at a different wavelength in the UV-visible spectrophotometer.

3.6 SODIUM NITROPRUSSIDE PROMOTED DEPHOSPHORYLATION OF PREFORMED COBALT (III) NITROPHENYLPHOSPHATE COMPLEXES AT 254NM UV IRRADIATION: PHOSPHATE DETERMINATION METHOD

2 mL of 5 x 10^{-3}M solution of 4-nitrophenylphosphate was mixed with the same amount of 5 x 10^{-3}M aqueous solution of $[Co(tn)_2(aq)]^{3+}$ in a thermostated reaction vessel and the volume made up to 10mL and pH adjusted to 7. The reaction produces a solution which is 1 x 10^{-3}M in $Cotn_2NPP$. Similarly addition of 2mL of 5 x 10^{-3}M aqueous solution of 4-NPP with 4 mL of 5 x 10^{-3}M aqueous solution of $[Co(tn)_2(aq)]^{3+}$ produces a solution which is 1 x 10^{-3}M in $Cotn_2NPP$ complex. Analogously, 2mL of 5 x 10^{-3}M aqueous solution of 4-NPPi with 6mL of 5 x 10^{-3}M aqueous solution of $[Co(tn)_2(aq)]^{3+}$ produces a solution which is 1 x 10^{-3}M in $Cotn_2NPP$ complex. After 5 minutes of reaction time, 2mL of 5 x 10^{-3}M aqueous solution of SNP, initial pH of 7 was added and irradiated at 254nm. Production of inorganic phosphate was monitored at 885nm using the protocol of study during the formation of the cobalt complexes (0-5 minutes) and after the resumption of the photolysis reaction by SNP (5-120 minutes). The results are shown in figure 3.5.

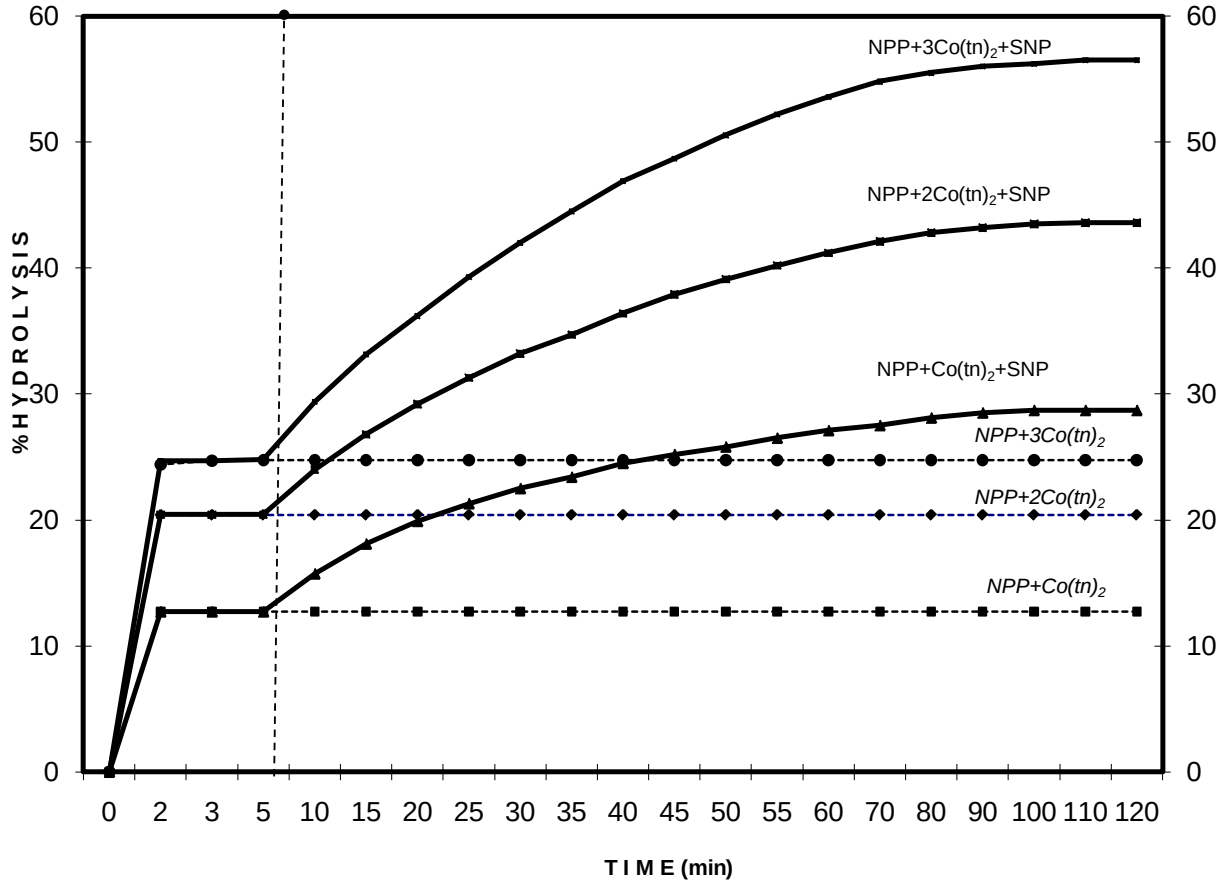

Figure 3.5 Percentage hydrolysis for the reaction of preformed 1 x 10^{-3}M $Cotn_2$NPP complexes (1:1, 2:1 and 3:1; $Cotn_2$: NPP ratio) with 1 x10^{-3}M aqueous solution of $Na_2[Fe(CN)_5NO]$ at 254nm and 25^{o}Cand initial pH of 7

The result shown in figure 3.5 using the phosphate determination method clearly showed slight difference and the effect of nitric oxide from its nitrophenolate counterpart in figure 3.2 when the cobalt complex is increased to 3:1 to the SNP. Again this reaction can be explained in two phases, the initial $Cotn_2$NPP complex formation where monodentate and chelated $Cotn_2$NPP prevail in the solution, with dephosphorylation initiated by coordinated water or hydroxyl radical and the increase in dephosphorylation activities triggered by the introduction of nitric oxide. This can be attributed to all the oxygen sites of the NPP being coordinated by the metal thereby more electron withdrawal from the phosphorus centre and possibly Le Chatelier's principle effects that drives the reaction forward.

3.7 THE EFFECT OF HIGHER MOLE RATIO OF SODIUM NITROPRUSSIDE AT 254NM IRRADIATION ON THE DEPHOSPHORYLATION OF PREFORMED COBALT (III) NITROPHENYLPHOSPHATE COMPLEXES: PHOSPHATE DETERMINATION METHOD

The amount of 5×10^{-3}M aqueous solution of $Na_2[Fe(CN)_5NO]$, (25^oC and initial pH of 7) to be added to the preformed cobalt nitrophenylphosphate complexes was increased to 4mL and 6mL to effectively produce 2:1 and 3:1 mole ratio of SNP to cobalt complexes. The production of inorganic phosphate was monitored accordingly. The results are depicted in figure 3.6.

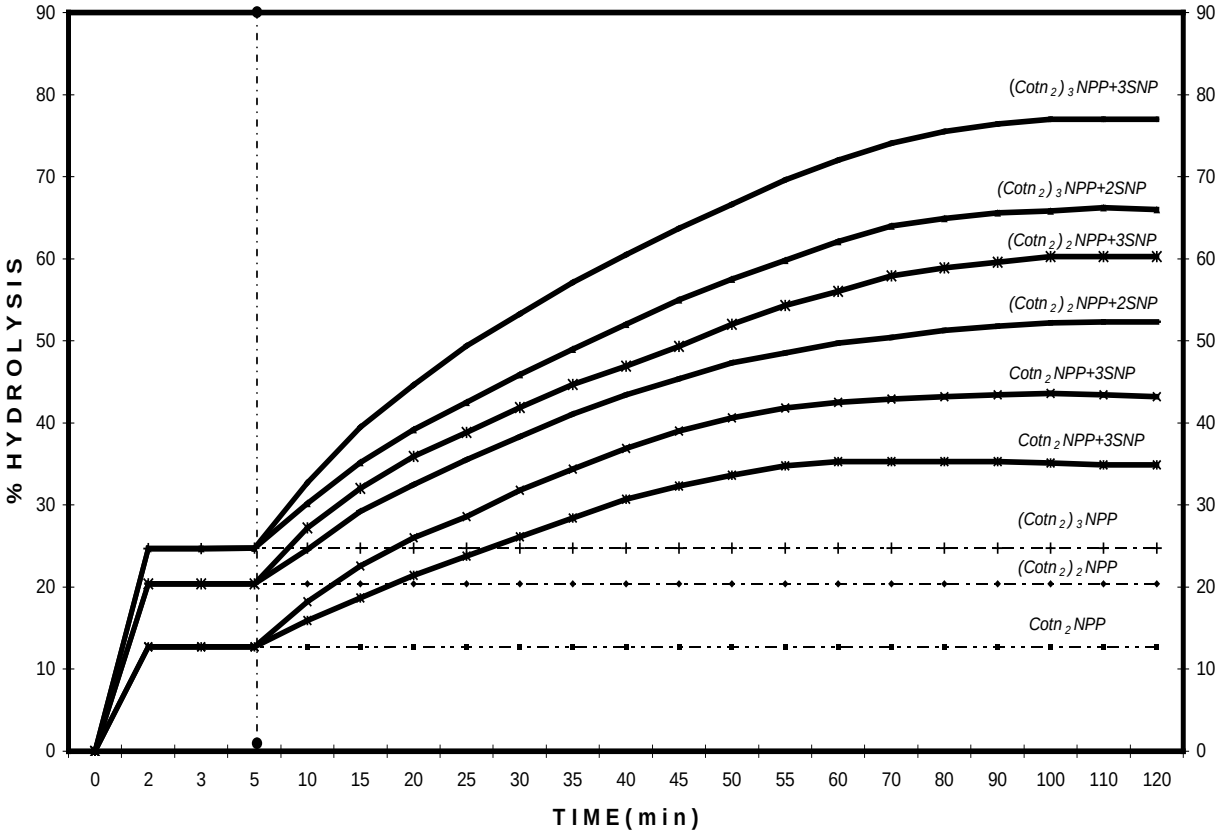

Figure 3.6 Percentage hydrolysis for the reaction of preformed 1 x 10^{-3}M $Cotn_2NPP$ complexes (1:1, 2:1 and 3:1; $Cotn_2$: NPP ratio) with 1 x 10^{-3}M aqueous solution of $Na_2[Fe(CN)_5NO]$ (1:1,2:1 and 3:1 molar ratios with respect to SNP and cobalt phosphate complexes) at 254nm irradiation (25^oc and initial pH of 7).

Higher mole ratios of nitric oxide were also used to conduct the experiment by increasing the SNP to 2 and 3 mole ratios to the $Cotn_2NPP$, $Co(tn_2)_2NPP$ and $Co(tn_2)_3NPP$ molar ratios. The result obtained for these reactions is shown in figure 3.6. It is noted that in all SNP increased systems, the dephosphorylation activities increases. This shows the effect of nitric oxide as an effective nucleophile for intermolecular attack on the phosphorus centre or an effective trigger for intramolecular attacks by coordinated water or hydroxyl of the metal complex.

3.8 SODIUM NITROPRUSSIDE ASSISTED DEPHOSPHORYLATION OF SODIUM PYROPHOSPHATE: PHOSPHATE DETERMINATION METHOD

The dephosphorylation reaction of 1×10^{-3}M aqueous solution of sodium pyrophosphate with an equimolar amount of aqueous sodium nitroprusside was studied under 254nm photolysis. A 2:1 and 3:1 molar ratio of SNP: PPi reaction solutions were also subjected to similar study. In these reactions the inorganic free phosphate produced as a result of dephosphorylation was monitored. The results and pH profile are shown in figure 3.7 below

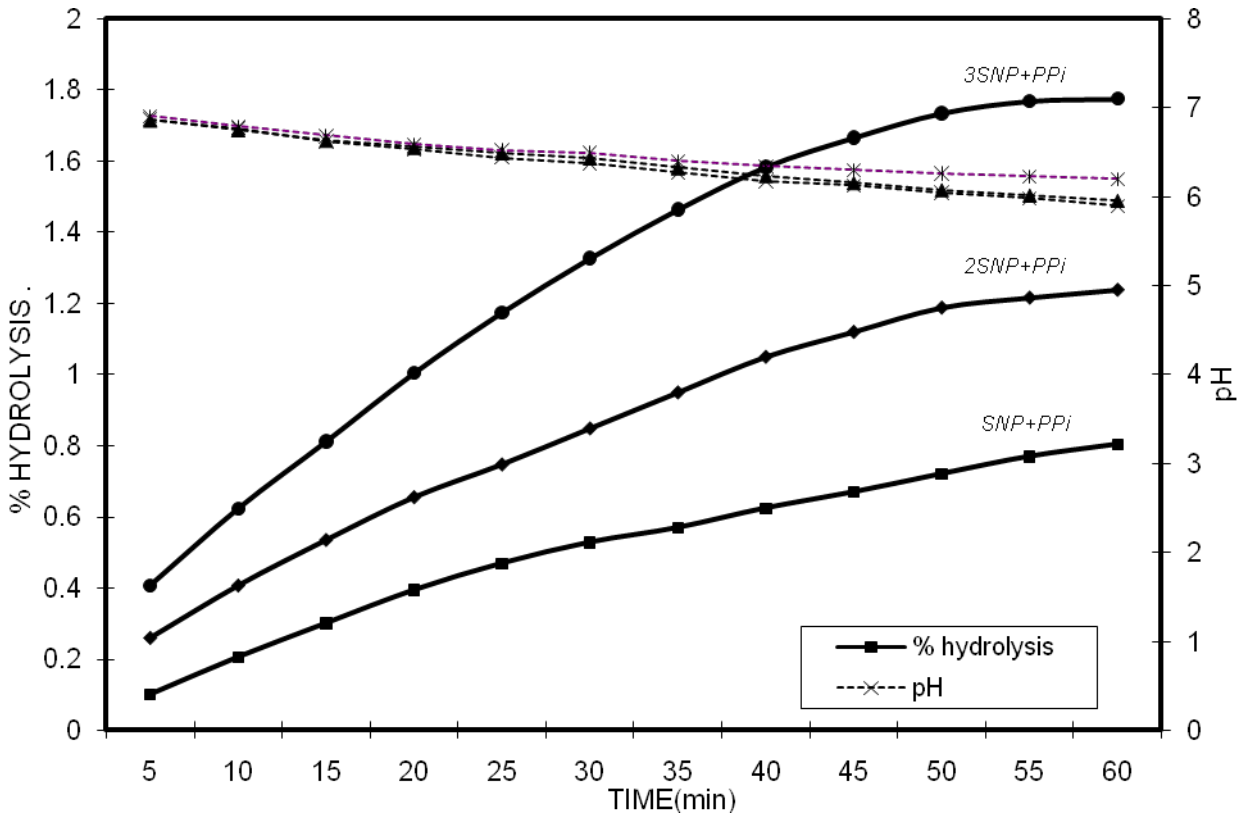

Figure 3.7 Percentage hydrolysis and pH profile for the reaction of 1 x 10^{-3}M aqueous solution of sodium pyrophosphate with 1 x 10^{-3}M aqueous solution of $Na_2[Fe(CN)_5NO]$ at 254nm for 1:1, 2:1 and 3:1 ; SNP:PPi ratio at 25^{o}C and initial pH of 7 using phosphate determination method.

So far we have recorded different reactivity and rate enhancement in our reactions with nitric oxide, $[Co(tn)_2(aq)]^{3+}$ and p-nitrophenylphosphate. The question still is, can the dephosphorylation results obtained be the same for all forms of phosphates, activated and unactivated? Nitrophenylphosphate is an activated phosphate; we then used sodium pyrophosphate as our simplest unactivated phosphate and subject it to similar experimental procedures in line with our protocol of study. This experiment was conducted by measuring the amount of inorganic phosphate produced in solution.

The results obtained for the reaction of the pyrophosphate with SNP is shown above in figure 3.7. In the experiment, we stoichiometrically increased the SNP to PPi ratio from 1:1 to 3:1, all initial pH of reactions starting from 7.0. The result showed little or no appreciable dephosphorylation as nitric oxide concentration is increased in the system.

When compared to figure 3.4 (reaction with nitrophenylphosphate), we can clearly see that there is an effect of activation of the phosphate in the previous experiment compared to the one done with the pyrophosphate.

3.9 SODIUM NITROPRUSSIDE PROMOTED DEPHOSPHORYLATION OF PREFORMED COBALT(III) PYROPHOSPHATE COMPLEXES AT 254NM UV IRRADIATION: PHOSPHATE DETERMINATION METHOD

2 mL of 5 x 10^{-3}M solution of sodium pyrophosphate was mixed with the same amount of 5 x 10^{-3}M aqueous solution of $[Co(tn)_2(aq)]^{3+}$ in a thermostated reaction vessel and the volume made up to 10mL and pH adjusted to 7. The reaction produces a solution which is 1 x 10^{-3}M in $Cotn_2PPi$. Similarly addition of 2mL of 5 x 10^{-3}M aqueous solution of PPi with 4 mL of 5 x 10^{-3}M aqueous solution of $[Co(tn)_2(aq)]^{3+}$ produces a solution which is 1 x 10^{-3}M in $Cotn_2PPi$ complex. Analogously, 2mL of 5 x 10^{-3}M aqueous solution of PPi with 6mL of 5 x 10^{-3}M aqueous solution of $[Co(tn)_2(aq)]^{3+}$ produces a solution which is 1 x 10^{-3}M in $Cotn_2PPi$ complex. After 5 minutes of reaction time, 2mL of 5 x 10^{-3}M aqueous solution of SNP, initial pH of 7 was added and irradiated at 254nm. Production of inorganic phosphate was monitored at 885nm using the protocol of study during the formation of the cobalt complexes (0-5 minutes) and after the resumption of the photolysis reaction by SNP (5-120 minutes). The results are shown in figure 3.8.

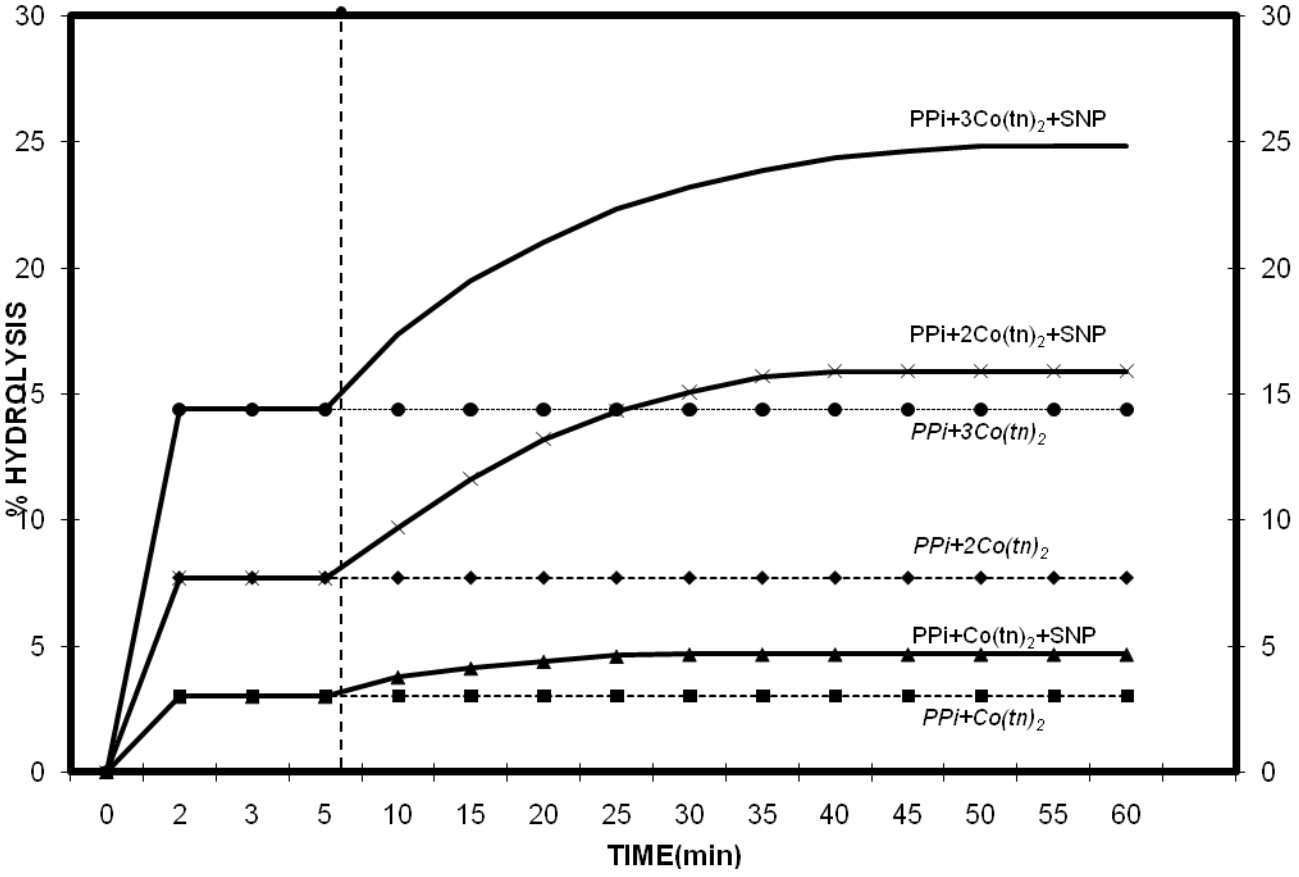

Figure 3.8 Percentage hydrolysis for the reaction of preformed 1 x 10^{-3}M $Cotn_2PPi$ complexes (1:1, 2:1 and 3:1; $Cotn_2$: PPi ratio) with 1 x10^{-3}M aqueous solution of $Na_2[Fe(CN)_5NO]$ at 254nm and 25^{o}Cand initial pH of 7 using the phosphate determination method.

Activation of the pyrophosphate was done by adding different mole ratio of $[Co(tn)_2(aq)]^{3+}$ to the pyrophosphate and the subsequent addition of the SNP followed with photolysis of the reaction solution. Figure 3.8 above depicts results obtained from this experiment. The reaction was noted to be biphasic, an initial dephosphorylation which levels off about 2-3 minutes of addition of the $[Co(tn)_2(aq)]^{3+}$ to the pyrophosphate and a steady gradual increase noted as SNP was added and solution irradiated (5-60 minutes) as shown in figure 3.7. Higher mole ratios of $[Co(tn)_2(aq)]^{3+}$, PPi and SNP showed same trend and increased results as they enzyme models are varied to the substrate models. The result of these experiments is shown in figure 3.9. Different species of the pyrophosphate coordination to cobalt complexes has been reported by Milburn et al [57] and Phosphorus-31 NMR was used to elucidate different activated species that can

be obtained in the reaction as shown below.

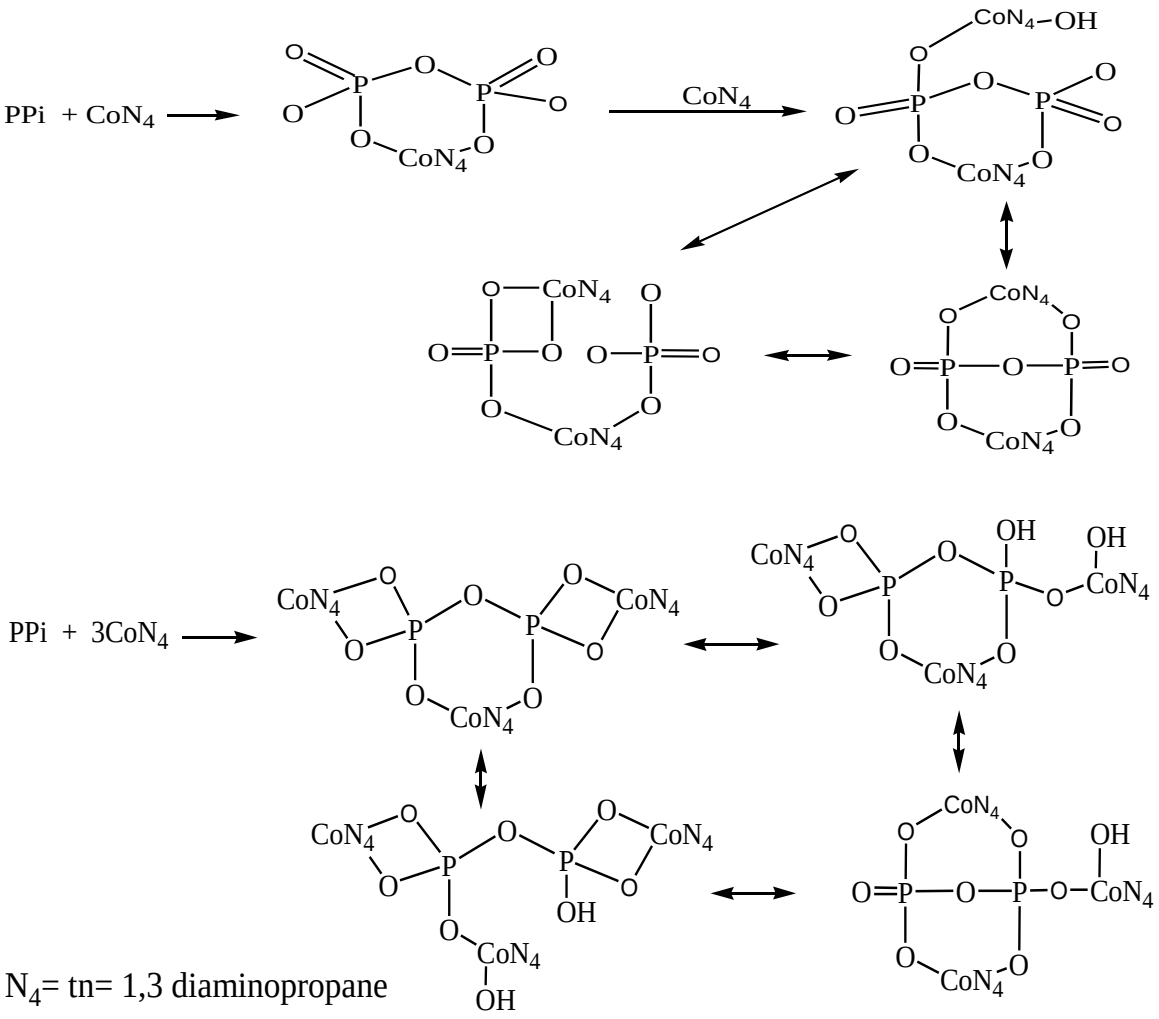

An increase in dephosphorylation was noted for systems that contained $Cotn_2PPi$ and nitric oxide compared to those that contained only PPi and nitric oxide. The chelation of the cobalt complex to PPi results in an activated species which is presumably prone to attack by a nucleophile such as water, coordinated hydroxide or nitric oxide on the phosphorus centre that result in the cleavage of the P-O-P bond leading to increased dephosphorylation observed in the different reactions. It can be seen from the results in figures 3.8 that more dephosphorylation reactions were recorded for systems containing more cobalt complexes. The structures above shows that there is more electron withdrawal from the phosphorus centre for higher cobalt complex to PPi ratios, thereby accounting for increased results obtained for such systems.

3.10 THE EFFECT OF HIGHER MOLE RATIO OF SODIUM NITROPRUSSIDE AT 254NM IRRADIATION ON THE DEPHOSPHORYLATION OF PREFORMED COBALT (III) PYROPHOSPHATE COMPLEXES: PHOSPHATE DETERMINATION METHOD

The amount of 5 x 10^{-3}M aqueous solution of $Na_2[Fe(CN)_5NO]$, (25^oC and initial pH of 7) to be added to the preformed cobalt pyrophosphate complexes was increased to 4mL and 6mL to effectively produce 2:1 and 3:1 mole ratio of PPi to cobalt complexes. The production of inorganic phosphate was monitored accordingly. The results are depicted in figure 3.9.

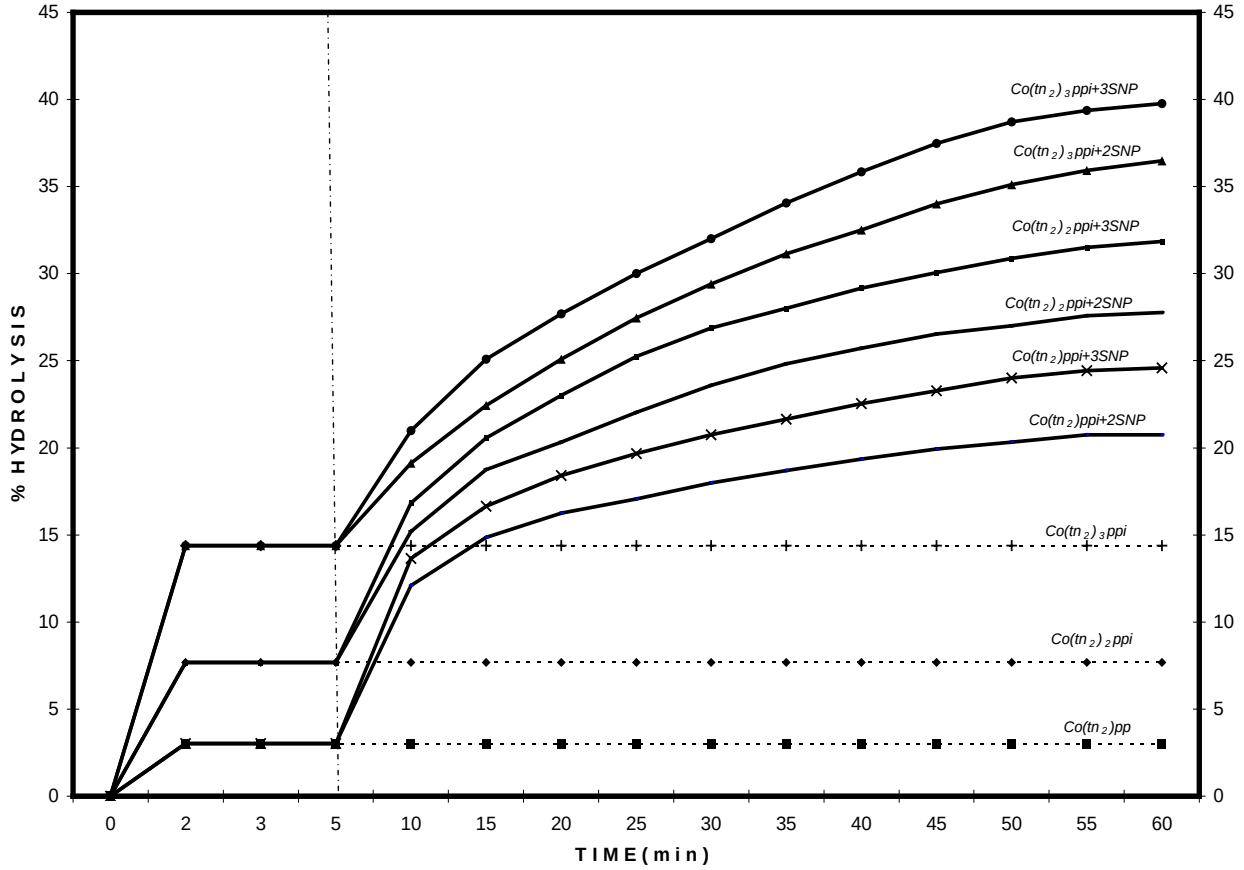

Figure 3.9 Percentage hydrolysis for the reaction of preformed 1 x 10^{-3}M $Cotn_2PPi$ complexes (1:1, 2:1 and 3:1; $Cotn_2$: PPi ratio) with 1 x 10^{-3}M aqueous solution of $Na_2[Fe(CN)_5NO]$ (1:1,2:1 and 3:1 molar ratios with respect to SNP and cobalt phosphate complexes) at 254nm irradiation (25^oc and initial pH of 7).

The result in figure 3.9 depicts effect of higher mole ratio of SNP to the $Cotn_2PPi$ complex. The SNP addition and irradiation after the formation of the $Cotn_2PPi$ complex effected more dephosphorylation results as can be seen by the percentage hydrolytic rate obtained. The amount of SNP in this reaction was doubled and tripled as compared to results obtained in figure 3.8. The above result showed steady increase in dephosphorylation as SNP was increased in reaction solution. It is worthy to note that hydrolytic rates obtained for higher mole ratios of SNP to $Cotn_2PPi$ were always lower than that of SNP to $Cotn_2NPP$ complexes in all the reactions. The effect of the activated phosphate of the NPP could be a possible explanation for the increased rate enhancement obtained over the PPi experiments. Activation of the phosphate withdraws electron from the phosphate center, increasing its positive charge for possible nucleophilic attack.

In all cases, the results obtained for PPi promoted by $[Co(tn)_2(aq)]^{3+}$ and nitric oxide was found to be less than those of NPP under similar conditions. We postulate that the nitrosated intermediates of PPi moieties hydrolyse via an intramolecular mechanism as advanced in the literature [102]. The nitrosated PPi will decompose to a metaphosphate intermediate and a nitrite followed by rapid hydration of the former back to pyrophosphate as shown below.

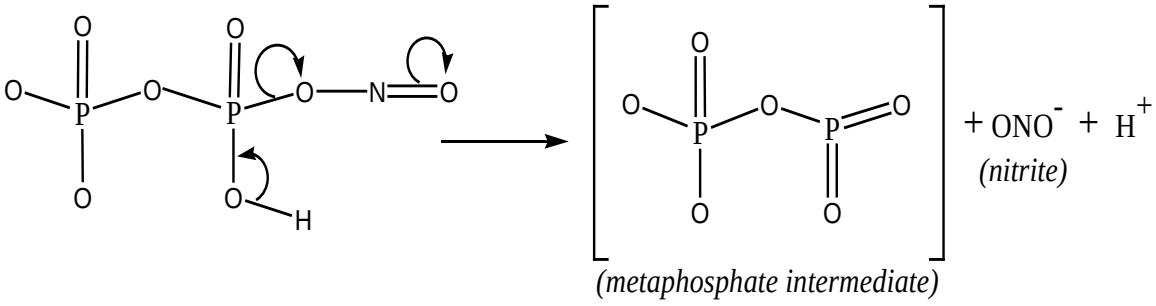

The above reaction can be a possible explanation to the low yield in dephosphorylation noted for the reaction between the pyrophosphate and nitric oxide shown in figure 3.7.
The reactions involving NPP and PPi with nitric oxide are presumably prone to nitrosation reactions. Shown below is a plausible nitrosation scheme for the reactions

involving nitric oxide solutions with phosphates in the presence of oxygen.

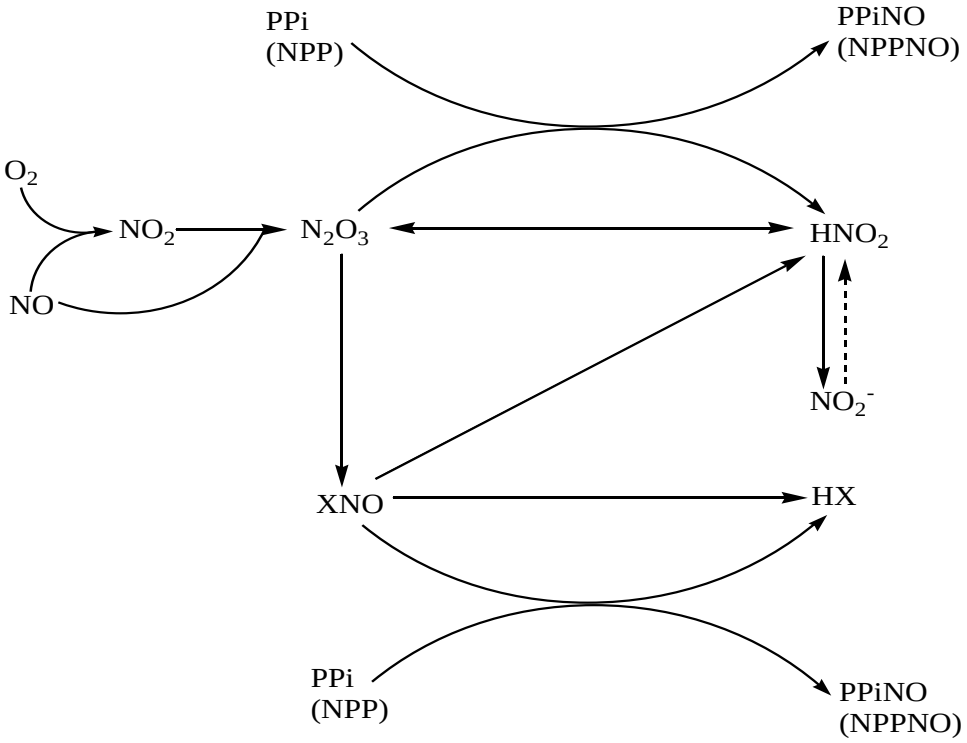

Scheme 3.1 Plausible nitrosation scheme for the reactions involving nitric oxide solutions with phosphates in the presence of oxygen. The dashed arrow applies only in acidic solutions. (X = various anions, NPP = nitrophenylphosphate, PPi = inorganic pyrophosphate

The reaction scheme for the nitrosation reaction of NPP and PPi at neutral pH could be explained as follows;

$2NO + O_2 \longrightarrow 2NO_2$ 25

$NO + NO_2 \rightleftharpoons N_2O_3$ 26

$N_2O_3 + H_2O \rightleftharpoons 2HNO_2 \rightleftharpoons 2NO_2^- + 2H^+$ 27

$N_2O_3 + NPP/PPi \longrightarrow NPPNO/PPiNO + NO_2^- + H^+$ 28

$$N_2O_3 + X^- \rightarrow XNO + NO_2^- \quad \text{.....29}$$

$$XNO + H_2O \rightleftharpoons HNO_2 + H^+ + X^- \rightleftharpoons NO_2^- + 2H^+ + X^- \quad \text{.....30}$$

$$XNO + NPP/PPi \longrightarrow NPPNO/PPiNO + H^+ + X^- \quad \text{.....31}$$

The above reactions have been used previously to describe nitrosation of amines by N_2O_3 under acidic conditions [103]. In our experimental condition of neutral pH, essentially all of the HNO_2 is completely dissociated to form NO_2^- (note that the pKa of nitrous acid is 3.36). This drives reaction (27) far to the right making NO_2^- a sink for N_2O_3 formed from the oxidation of NO (reactions 25 and 26). N_2O_3 can also react with anions in the solution as shown in equation (29), forming nitrosyl compounds which can themselves act as nitrosating agents depicted in equations (30) and (31).

CHAPTER FOUR

4.0 CONCLUSION

Nitrates and nitrites are usually present in the environment. The irradiation of nitrate is responsible for the environmental presence of nitrite. Due to the generation of hydroxyl radicals, the photolysis of nitrate and nitrite can lead to the degradation of organic compounds [104]. This effect can result in decontamination induced by photolytic processes in the environment leading to photo induced degradation of organic pollutants including the poorly biodegradable phosphate ester contaminants. The role of the direct reaction of nitric oxide with the organophosphate moiety in this decontamination process has been overlooked. Our investigation depicts the active role that played by oxides of nitrogen in the degradation of nitrophenylphosphate/sodium pyrophosphate which are modelled as organophosphate substrates. The presence of metal ions such as iron in the environment will presumably aid in the formation of metal chelates with the phosphate esters thereby resulting in synergistic cooperativity towards the dephosphorylation reactions promoted by nitric oxide in line with the findings of our study.

In this study, the direct participation of nitric oxide in the dephosphorylation (decontamination) of phosphate esters was realised and the following observations were noted in this study which will serve as a yardstick for further studies;

(a) Dephosphorylation reactions of nitrophenylphosphate/sodium pyrophosphate using SNP as nitric oxide donor at high concentrations of enzyme/substrate ratios is best monitored using the phosphate determination method.

(b) Activation of the phosphate moiety is essential for effective dephosphorylation by nitric oxide as shown by this study, as direct reaction of pyrophosphate with nitric oxide did not yield positive results.

(c) There appears to be synergistic cooperativity between metal ions and nitric oxide in dephosphorylation reactions.

(d) The effect of nitric oxide dephosphorylation is presumed to be brought about by a combination of factors that includes hydroxyl radicals, nitric oxide, metal ions etc in the biosphere.

This study also looks at the environmental implications of the use of organophosphate esters in form pesticides, fertilizers and warfare agents to mention but a few and suggests practical approach to the effective curbing or destruction of these useful but nevertheless harmful substances in the environment. It shows that dephosphorylation reaction involving nitric oxide and oxides of nitrogen occurs daily in nature and this study should serve as a yardstick in proposing decontamination formulations that can be useful in our biosphere. The search for a suitable or modest decontamination solution should be of paramount importance, because organophosphate esters are daily used in one form or the other in our daily lives. Great efforts has been made by most developed countries to put structures in place and organised destructive sites where organophosphate wastes are treated, destroyed or possibly recycled. The problem still lies in the developing countries that are predominantly rural and are plagued with acute shortage of food and wide spread of insect borne diseases such as malaria, yellow fever, dengue fever etc. Most countries are predominantly war-stricken and the application of nerve agents in war situations is continually on the rise. In fact, the search for effective decontamination solution is a global problem. Substandard and sometimes expired pesticides, fertilizers and herbicides which are mainly organophosphate formulations are widely used in most part of the world to increase acute food shortage and to curb prevalent environmental pests. Sometimes lack of technical know-how on the application of these chemicals constitutes the regular abuse of organophosphate esters in the form of unregulated and improper usage. Decontamination formulations are of paramount important in most area of the world and such formulations should take into account the condition of usage and the prevalent environmental conditions such as temperature and humidity of the intended regions where these chemicals are to be used.

Most phosphate deposits in the environment are as a result of human activities. Phosphate concentration increase in surface waters enhances the growth of aquatic plant life. Run-off from fertilized farm lands can stimulate plant growth in lakes and streams. Waste

water that contains phosphates from detergents can have the same effect. Lakes that are rich in plant nutrients suffer from accelerated eutrophication. When the lush aquatic plant growth in a nutrient-rich lake dies, the decomposition of the dead plant material consumes dissolved oxygen. This consumption reduces the level of dissolved oxygen to a point where it is insufficient to support animal life. To reduce the threat of lake eutrophication, many localities have banned the use of phosphates in detergents. In some cases, the phosphates have been replaced by carbonates. In others, new detergents have been developed that do not react with the Ca^{2+} and Mg^{2+} ions of hard water.

Furthermore, organophosphate compounds are of interest to many groups of chemists. Biochemists study their relationship to cholinesterase inhibition in mammals, organic chemists investigate their reaction mechanisms to improve synthetic routes to these chemicals, and environmental chemists are interested in these compounds due to their roles as pesticides, as well as their persistence and overall toxicity in the environment. They are widely used for the elimination of crustaceans and mosquitoes. They also find uses in the heavy industries as hydraulic fluid additives and in the petrochemical industries as plasticizers and they are very important constituents of most commercially produced fertilizers.

Despite the extensive production and resultant widespread exposure of environmental compartments to various amounts of these compounds, surprisingly few quantitative data on their hydrolytic reactivity are reported in open literature. This lack of information is particularly surprising because hydrolytic transformation is proposed as an important pathway for the degradation of these compounds in the ecosystem [105]. This study has established efficient functional models which have made understanding the facile degradation of toxic organophosphate esters (pesticides and chemical warfare nerve agents) in the biosphere easy. Formulations that require less logistic support, that have minimal runoff of fluids and in effect no lasting impact on the environment can be recommended in decontamination model solution. This investigation was achieved under mild conditions and requires no specialized equipment and can be adapted in the developing countries that lack expertise and technical know-how of the advanced countries. Adapting these dephosphorylation methods in vivo using real environmental

hazardous substances is recommended and should be a subject for further research. Utilizing organised assemblies such as microemulsions and miscelles should also be a subject of further investigation. Microemulsions are generally ternary fluid made up of an aqueous phase, an oil phase, a surfactant and cosurfactant. They are quite unique in their ability to form a single phase of low viscosity and low interfacial tension with excess oil or water.

REFERENCES

(1) S.C.L Kamerlin, J. Wilkie; The role of metal ions in phosphate ester hydrolysis, Org. Biomol. Chem. 5(13), (2007) 2098-2108.

(2) F. Aguilar-Perez, P. Gomez-Tagle, E. Collado-Fregoso, A.K. Yatsimirsky; Phosphate ester hydrolysis by hydroxo complexes of trivalent lanthanides stabilized by 4-imidazolecarboxylate, Inorg. Chem. 45(23), (2006) 9502-9517.

(3) S. Parimala, M. Kandaswamy; Synthesis, characterization and electrochemical behavior of mononuclear, binuclear nickel (II) and heterobinuclear zinc(II)nickel(II) complexes derived from novel macrobicyclic tricompartmental ligands: kinetics of the catalytic hydrolysis of 4-nitrophenyl phosphate by the complexes, Transit. Metal Chem. (Dordrecht, Netherlands) 29(1), (2004) 35-41.

(4) B.G. Kotak, S.L. Kenefick, D.L. Fritz, C.G. Rousseaux, E.E. Prepas, S.E. Hrudley; Occurrence and toxicological evaluation of cyanobacterial toxins in Alberta lakes and farm dugouts, Water Res. 27(3), (1993) 495-506.

(5) F. Tafesse; Hydroxoaquotetramine cobalt(III) promoted hydrolysis of pyrophosphate, Mechanistic considerations, Transit. Metal Chem. 16(1991) 114-118.

(6) F. Tafesse; Comparative studies on Prussian blue or diaaquatetraamine cobalt(III) promoted hydrolysis of 4-nitrophenylphosphate in microemulsions, Int. J. Mol. Sci. 4, (2003) 362-370.

(7) F. Tafesse, K. Eguzozie; Efficient hydrolysis of 4-nitrophenylphosphate catalysed by copper bipyridyl in microemulsion, Ecotox. Environ. Safe. (2008) doi: 10.1016/ J.ecoenv. 2008.01.010.

(8) F. Tafesse, K. Eguzozie; Model chemical decontamination studies of phosphate esters in aqueous and microemulsion media, Synth. React. Inorg. Me. 38:6, (2008) 484-490.

(9) M.J. Coye, P.G. Barnett, A.R. Valesco, P. Romero, C.L. Clements, T.G Rose; Clinical confirmation of organophosphate poisoning by serial cholinesterase analyses, Arch. Intern. Med. 3(147), (1987) 438-442.

(10) J.B. Sullivan, J Blose; Organophosphate and carbamate insecticides; Hazardous material toxicology. Clinical principles of environmental health, Baltimore. Williams and Wilkins (1992) 1015-1026.

(11) S.W. Wiener, R. Hoffmann; Nerve agents: a comprehensive review, J. Intensive Care Med. 19(1), (2004) 22-37.

(12) T. Okumura, T. Nobukatsu, S. Ishimatsu; Report on 640 victims of the Tokyo Subway Sarin Attack, Ann. Emerg. Med. 28, (1996) 129-135.

(13) M. Amitabha, A.A David et al; Group 13 chelates in nerve gas agent and pesticide deakylation, New J. Chem., DOI: 10.1039/B717041f (2008) 1-6.

(14) K.U. Eguzozie, (M.Sc. Dissertation), Metal ion mediated hydrolysis of 4-nitrophenylphosphate in microemulsion media: catalytic vs stoichiometric effect (2008) 3-6.

(15) J. Emley, D. Hall; Biophosphorus Chemistry, 3rd Edition (1976) 93-99.

(16) F.H. Westheimer; Why nature chose phosphates, Science 235 (4793), (1987) 1173-1178.

(17) S.P. Graham, R.S. Magee; Critical evaluation of proven chemical weapon destruction technologies (IUPAC technical report), Pure Appl. Chem. 74(2), (2002) 187-316.

(18) T.A. Slotkin, F.J. Seidler; Comparative developmental neurotoxicity of organophosphates in vivo: Transcriptional responses of pathways for brain cell development, cell signalling, cytotoxicity and neurotransmitter systems. Brain Res. Bull. 72, (2007) 232-274.

(19) H.F. Bondy, J.P.W. Hughes, J.L. Leahy, A.N. Worden; Effects of triaryl-phosphates on cholinesterase, Toxicology 1(2), (1973) 143-150.

(20) M.J. Nevins, W.W. Johnson; Acute toxicity of phosphate ester mixtures to invertebrates and fish, B. Environ. Contam. Tox. Springer-verlag, N.Y. 19(2), (1978) 250-256.

(21) T. Wagner-Jauregg, B.E. Hackley Jr, T.A. Lies, O.O. Owens, R. Proper; Model reactions of phosphorus containing enzymes inactivators IV, The catalytic activity of certain metal salts and chelates in the hydrolysis of diisopropylfluorophosphates, J. Am. Chem. Soc. 77, (1955) 922-929.

(22) F. Tafesse; Hydrolysis of 4-nitrophenyl phosphate in microemulsions assisted by polymetallic complexes: A bio-mimetic model for decontamination of organophosphate pollutants.,Synth. React. Inorg. Me. (35) 8, (2005) 645-650.

(23) J. Chin; Developing artificial hydrolytic metalloenzymes by a unified mechanistic approach, Acc. Chem. Res. 24, (1991) 145-152.

(24) K. Lai, K.I. Dave, J.R. Wild; Bimetallic binding motifs in organophosphorus hydrolase are important for catalysis and structural organization, J. Biol. Chem. 269(24), (1994) 16579-16584.

(25) W.B. Knight, D. Dunaway-Mariano, S.C. Ransom, J.J. Villafranca; Investigations of the metal ion-binding sites of yeast inorganic pyrophosphates, J. Biol. Chem. 259(5), (1984) 2886-2895.

(26) F. Ramirez, J. Marecek, J. Minore , S. Srivastava, W. Le Noble; On the freeness of the metaphosphate anion in aqueous solution, J. Am. Chem. Soc. 108(2), (1986) 348-349.

(27) F.H. Westheimer; Monomeric metaphosphates in enzymic and in enzyme-model systems, ACS Sym. Ser. 171(Phosphorus Chem.), (1981) 65-68.

(28) A. Smilkjo; Chemical kinetics and inorganic reaction mechanisms, 2nd edition, Springer, (2003) 40-41.

(29) F. Ramirez, J. F. Marecek; Coordination of magnesium with adenosine 5'-diphosphate and triphosphate. Biochim. Biophys. Acta. 589(1), (1980) 21-29.

(30) Z. Zhong-yin; Protein tyrosine phosphatases: structure and function, substrate specificity, and inhibitor development, Annu. Rev. Pharmacol. 42, (2002) 209.

(31) D. Barford; Molecular mechanisms of the protein serine/threonine phosphatases Trends Biochem. Sci. 21(11), (1996) 407.

(32) D. Gani, W. John; Metal ion in the mechanism of enzyme-catalysed phosphate monoester hydrolyses, Struct. Bond. 89, (1997) 133-174.

(33) R.L. Van Etten; Human prostatic acid phosphatase: a histidine phosphatise, Ann. N.Y. Acad. Sci. 390, (1982) 27-51.

(34) S.L. Buchwald, M.S. Saini, J.R. Knowles, R.L. Van Etten; Stereochemical course of phosphor group transfer by human prostatic acid phosphatise, J. Biol. Chem. 259(4), (1984) 2208-2213.

(35) R.L. Van Etten, J.M. Risley; Phosphate (oxygen)-water exchange reaction catalyzed by human prostatic acid phosphatase. P. Natl. Acad. Sci. U.S.A. 75(10), (1978) 4784 -4787.

(36) L.A. Fothergill-Gilmore, H.C. Watson; The phosphoglycerate mutases, Adv. Enzymol. R.A.M.B. 62, (1989) 227-313.

(37) L.G. Butler; The enzymes. 3rd Ed, Boyer PD (Ed.) Academic Press N.Y. 4, (1971) 529-541.

(38) W.B. Knights, S.W. Fitts, D. Dunaway-Mariano; Investigation of the catalytic mechanism of yeast inorganic pyrophosphate, Biochemistry. 20(14), (1981) 4029-4086.

(39) E.A. Merritt, M. Sundaralingam; Models of metal-nucleoside polyphosphates: structures of unidentate $[CoHP_2O_7(NH_3)_5].H_2O$ [Pentaamminepyrophosphatocobalt (III) monohydrate] and bidentate $[CoHP_2O_7(NH_3)_4].2H_2O$ [tetraamminepyrophosphatocobalt (III) dihydrate**],** Acta. Crystallogr. B: Structural Crystallography and Crystal Chemistry B36 (11), (1980) 2576-2584.

(40) K.M. Welsh, I.M. Armitage, B.S. Cooperman; Yeast inorganic pyrophosphatase. Functional and $^{113}Cd^{2+}$ and ^{31}P nuclear magnetic resonance studies of the Cd^{2+} enzyme. Biochemistry. 22(5), (1983) 1046-1054.

(41) W.B. Knight, S.J. Ting, S. Chuang, D. Dunaway-Mariano, T. Haromy, M. Sundaralingam ; Yeast inorganic pyrophosphatase substrate recognition, Arch. Biochem. Biophys. 227(1), (1983) 302-309.

(42) E.A. Merritt, M. Sundaralingam, D. Dunaway-Mariano; Crystal structure and chelate ring pucker of bidentate(pyrophosphate) tetraaquochromium(III) trihydrate, a model for metal-ADP coordination. J. Am. Chem. Soc. 103(12), (1981) 3565-3567.

(43) B.S. Cooperman; Methods in Enzymology. Purich DL(Ed), Academic Press N.Y. 82, (1982) 526-548.

(44) B.C. Antanaitis, P. Aisen; Uteroferrin and the purple acid phosphatises, Adv. Inorg. Biochem. 5, (1983) 111-136.

(45) B.C. Antanaitis, P. Aisen; Stoichiometry of iron binding by uteroferrin and its relationship to phosphate content, J. Biol. Chem. 259(4), (1984) 2066-2069.

(46) B.P. Gaber, J.P. Sheridan, F.W. Bazer, R.M. Roberts; Resonance Raman Scattering from uteroferrin, the purple glycoprotein of the porcine uterus. J. Biol. Chem. 254(17), (1979) 8340-8342.

(47) J.M. Halleen, H. Kaija, J.J. Stepan, P. Vihko, H.K. Vaananen; Studies on the protein tyrosine phosphatase activity of tartrate-resistant acid phosphatase. Arch. Biochem. Biophys. 352(1), (1998) 97-102.

(48) T. Klabunde, N. Strater, R. Frohlich, H. Witzel, B. Krebs; Mechanism of Fe(III)-Zn(II) purple acid phosphatise based on crystal structures. J. Mol. Biol. 259(4), (1996) 737-748.

(49) R. Itoh; IMP-GMP 5'-nucleotidase, Comp. Biochem. Phys. B, 105(1), (1993) 13-19.

(50) D. Gani, C.P. Downes, I. Batty, J. Bramham; Lithium and myo-inositol homeostasis B.B.A- Mol Cell Res. 1177(3), (1993) 253-269.

(51) A.P. Leech, G.R. Baker, J.K. Shute, M.A. Cohen, D.Gani; Chemical and kinetic mechanism of the inositol monophosphatase reaction and its inhibition by Li+, Eur. J. Biochem. FEBS 212(3), (1993) 693-704.

(52) A.J. Ganzhorn, M.C. Chanal; Kinetic studies with myo-inositol monophosphatase from bovine brain, Biochemistry 29(25),(1990) 6065-6071.

(53) M. Cohn, N. Shih, J. Nick; Reactivity and metal-dependent stereospecificity of the phosphorothioate analogs of ATP in the arginine kinase reaction. Structure of the metal-nucleoside triphosphate substrate. J. Biol. Chem. 257(13), (1982) 7646-7649.

(54) E.K. Jaffe, J. Nick, M. Cohn; Reactivity and metal-dependent stereospecificity of the phosphorothioate analogs of ADP and ATP and reactivity of Cr (III) ATP in the 3-phosphoglycerate kinase reaction. Structure of the metal nucleotide substrates, J. Biol. Chem. 257(13), (1982) 7650-7656.

(55) D.R. Jones, L.F. Lindoy, A.M. Sargeson: Hydrolysis of phosphate esters bound to cobalt (III). Kinetics and Mechanisms of intramolecular attack by hydroxide on coordinated 4-nitrophenylphosphate, J. Am. Chem. Soc. 105(25), (1983) 732-733.

(56) D.S. Baldwin, J.K. Beattie, L.M. Coleman, D.R. Jones; Phosphate ester hydrolysis mediated by mineral phases, Environ. Sci. Technol. 29(6), (1995) 1706-1709.

(57) P.W.A. Hubner, R.M. Milburn; Hydrolysis of pyrophosphate to orthophosphate promoted by Co(III). Evidence for the role of polynuclear species, Inorg. Chem. 19, (1980) 1267-1272.

(58) G.A. Abbott; The rate of hydration of pyrophosphoric acid in aqueous solution, J. Am. Chem. Soc. 31, (1909) 763-770.

(59) J.R. Van Waser, Phosphorus and its compouds, Wiley interscience, New York, (1958), Volumes I and II.

(60) H. Sigel, F. Hofstetter; Metal-ion-promoted dephosphorylation of the 5'-triphosphates of uridine and thymidine, and a comparison with the reactivity in the corresponding cytidine and adenosine nucleotide systems, Eur. J. Biochem. FEBS 132(3), (1983) 569-577.

(61) B. Anderson, R.M. Milburn, J.M. Harrowfield, G.B. Robertson, A.M. Sargeson; Cobalt (III) promoted hydrolysis of a phosphate ester, J. Am. Chem. Soc. 99(8), (1977) 2652-2661.

(62) C.C. Addison, J. Lewis; The chemistry of the nitrosyl group (NO), Quart. Rev. Chem. Soc. 9, (1955) 115-149.

(63) W.A. Eric, M.A. Brodie; Nitric oxide - some new and old perspectives, J. Chem.Educ. 72(8), (1995) 686-692.

(64) L.J. Ignarro; Heme-dependent activation of soluble guanylate cyclase by nitric oxide: regulation of enzyme activity by porphyrins and metalloporphyrins, Semin. Hematol. 26(1), (1989) 63-76.

(65) H. Azuma, M. Ishikawa, S. Sekizaki; Endothelium-dependent inhibition of platelet aggregation, Brit. J. Pharmacol. 88(2), (1986) 411-415.

(66) B. Furlong, A.H. Henderson, M.J. Lewis, J.A. Smith; Endothelium-derived relaxing factor inhibits in vitro platelet aggregation, Brit. J. Pharmacol. 90(4), (1987) 687-692.

(67) J. Garth-Waite; Glutamate, nitric oxide and cell-cell signalling in the nervous system. Trends Neurosci.14 (2), (1991) 60-67.

(68) L. Stryer; Cyclic GMP cascade of vision, Annu. Rev. Neurosci. 9, (1986) 87-119.

(69) L.J. Ignarro, H. Lippton, J.C. Edwards, W.H. Baricos, A.L. Hyman, P.J. Kadowitz, C.A. Gruetter; Mechanism of vascular smooth muscle relaxation by organic nitrates, nitrites, nitroprusside and nitric oxide: evidence for the involvement of S-nitrosothiols as active intermediates, J. Pharmacol. Exp. Ther. 218(3), (1981) 739-749.

(70) M.A. Marletta, P.S. Yoon, R. Iyengar, C.D. Leaf, J.S. Wishnok; Macrophage oxidation of L-arginine to nitrite and nitrate: nitric oxide is an intermediate. Biochemistry. 27(24), (1988) 8706-8711.

(71) D.S. Bredt, S.H. Snyder; Isolation of nitric oxide synthetase, a calmodulin-requiring enzyme, P. Natl. Acad. Sci-Biol. 87(2), (1990) 682-685.

(72) D. Vione, V. Maurino, C. Minero, E. Pelizzetti; Reactions induced in natural waters by irradiation of nitrate and nitrite ions, Hand. Environ. Chem. 2(Pt. M), (2005) 221-253.

(73) I. Wagner, H. Strehlow, G. Busse; Flash photolysis of nitrate ions in aqueous solution, Z. Phys. Chem. (Muenchen, Germany) 123(1), (1980) 1-33.

(74) W.R. Haag, J. Hoigne; Kinetics and products of the reactions of ozone with various forms of chlorine and bromine in water, Ozone-Sci. Eng. 6(2), (1984) 103-114.

(75) R. Schwarz, K. Tede; Photochemistry of complex compounds. III. The hexacyano-complexes of tervalent iron, cobalt, chromium and manganese, Ber. Deut. Chem. Gesell. [Abteilung] B: Abhandlungen 60B (1927) 69-72.

(76) D.A. Foucher, D.H. Macartney, L.J. Warrack, J.P. Wilson; Kinetics and Mechanism of Ligand Substitution Reactions of Pentacyanoferrate (II) Complexes with Bridging N-Heterocyclic Dications in Aqueous Media, Inorg. Chem. 32, (1993) 3425-3432.

(77) F. Tafesse, M. Enemchukwu; Nitric oxide assisted hydrolysis of Nitrophenyl-phosphate, Nitric Oxide- Biol. Ch. 18(4), (2008) 274-278.

(78) R.P. Mitra, D.V.S. Jain, A.K. Banerjee, K.V.R. Chari; Photolysis of sodium nitroprusside and nitroprussic acid, J. Inorg. Nucl.Chem. 25(10), (1963) 1263-1266.

(79) A.C. Van Loenen, W. Hofs-Kemper; Stability and degradation of sodium Nitroprusside (2), Experimental. Pharma. Weekblad. 1(2), (1979) 424-436.

(80) W.I.K. Bisset, A.R. Butler, C. Glidewell, J. Reglinski; Sodium nitroprusside and cyanide release: Reasons for reappraisal, Brit. J. Anaesth. 53(10), (1981) 1015-1018.

(81) H.E. Spiegel, V. Kucera; Some aspects of sodium nitroprusside reaction with human erythrocytes, Clin. Chem. 23(12), (1977) 2329-2331.

(82) R.P. Mitra, B.K. Sharma, S.P. Mittal; Photolysis of sodium nitroprusside in the presence and absence of air, J. Inorg. Nucl. Chem. 34(12), (1972) 3919-3920.

(83) S.K. Wolfe, J.H. Swinehart; Photochemitry of pentacyanonitrosylferrate (2), Nitroprusside, Inorg. Chem. 14, (1975) 1049-1053.

(84) J.H. Espenson, S.G. Wolenuk; Kinetics and mechanism of some substitution reactions of pentacyanoferrate (III) complexes, Inorg. Chem. 11(9), (1972) 2034-2041.

(85) G. Stochel, R. Van Eldik, Z. Stasicka; Mechanistic information from medium- and high-pressure effects on the photooxidation of nitrosylpentacyanoferrate (II), Inorg. Chem. 25(20), (1986) 3663-3666.

(86) M.G. Oliviera, G.J. Langley, A.J. Rest; Photolysis of the $[Fe(CN)_5(NO)]^{2-}$ ion in water and poly(vinyl alcohol) films: evidence for cyano radical, cyanide ion and nitric oxide loss and redox pathways, J. Chem. Soc. Dalton Trans. (1995) 2013-2019.

(87) Spectroline Technical Bulletin; ultraviolet light Bulletin no 32. www.spectroline.com.

(88) H.F. Bauer, W.C. Drinkard; A general synthesis of cobalt(III) complexes. A new intermediate, $Na_3[Co(CO_3)_3].3H_2O$, J. Am. Chem. Soc. (1960) 825031-825032.

(89) J. Springborg, C.E. Schaffer; A new method for the preparation of dianionobis (diamine) cobalt (III) complexes, Acta. Chem. Scand. 27, (1973) 2223-2225.

(90) M. Halmann; Analytical chemistry of phosphorus compounds, John Wiley and sons. N.Y: Ed (1972) 248.

(91) V.L. Snoeyink, D. Jenkins; Water chemistry, John Wiley and sons N.Y. (1982) 299.

(92) J.N. Barrows, G.B. Jameson, M.T. Pope; Structure of a heteropoly blue: The four electron reduced beta-12-molybdophosphate anion, J. Am. Chem. Soc. 107, (1985) 1771.

(93) N.N. Greenwood, A. Earnshaw; Chemistry of the elements, Oxford: Butterworth Heinemann, 2nd edition, (1997) 23.

(94) J.C. Bailar Jr; The chemistry of the coordination compounds, Reinhold publishing corporation, (1956) 472-482.

(95) L.C.W. Baker, J.S. Figgis; A new fundamental type of inorganic complex: Hybrid between heteropoly and conventional coordination complexes. Possibilities for geometrical isomerism in 11-, 12-, 17- and 18- heteropoly derivatives, J. Am. Chem. Soc. 92(12), (1970) 3794-3797.

(96) J. Ramirez-Munoz; The colorimetric determination of phosphates in water at low ppm levels by automatic discrete sample analysis, Anal. Chim. Acta. 78, (1975) 431- 438.

(97) L.P. Khun, J.O. Doali, C. Wellman; The reaction of nitric oxide with

triethylphosphate, J. Am. Chem. Soc. 82, (1960) 4792–4794.

(98) S. Gallot, O. Thomas; Fast and easy interpretation of a set of absorption spectra: Theory and qualitative applications for UV examination of waters and waste waters, Fresen. J. Anal. Chem. 346 (1993) 976-983.

(99) C.A. Tolman, P.Z. Meakin, D.L. Linder, J.P. Jesson; Triarylphosphine, hydride and ethylene complexes of rhodium(I) chloride, J. Am. Chem. Soc. 96, (1974) 2762-2764.

(100) S.S. Massoud, R.M. Milburn; Determination of the acid dissociation constants of coordinated water in cis-diaquabis(1-3 diaminopropane) cobalt(III) ion, Inorg. Chim. Acta. 146 (1988) 3-4.

(101) D.R. Stranks, N. Vanderhoek; Effect of pressure on the isomerisation rate of the diaquobis(ethylenediamine) cobalt(III) ion, Inorg. Chem. 15(11), (1976) 2762-2764

(102) E.G. Demaster, B.J. Quast, R.A. Mitchell; Inhibition of S-nitrosation of reduced glutathione in aerobic solution of nitric oxide by phosphate and other inorganic anions, Biochem. Pharmacol. 53, (1997) 581-585.

(103) B.C. Challis, S.A. Kyrtopoulos; Rapid formation of carcinogenic N-nitrosamines in aqueous alkaline solutions, Brit. J. Cancer, 35(5), (1977) 693-696.

(104) D. Kotzias, H. Parlar, F. Korte; Photoreactivity of organic chemicals in water in the presence of nitrate and nitrite, Naturwissenschaften, 69, (1982) 444-445.

(105) S.D. Faust; Chemical hydrolysis of some organic phosphorus and carbamate pesticides in aquatic environments. Environ. Lett. 3(3), (1972) 171-201.